Transport of Pb and Zn by carboxylate complexes in basinal ore fluids and related petroleum-field brines at 100 °C: the influence of pH and oxygen fugacity

Thomas H. Giordano

Department of Geological Sciences, New Mexico State University, MSC 3AB, Las Cruces NM 88003. E-mail: tgiordan@nmsu.edu; Fax: (505) 646-1056; Tel: (505) 646-2511/2708

Received 9th May 2002, Accepted 31st July 2002
Published on the Web 16th September 2002

Article

It is well established through field observations, experiments, and chemical models that oxidation (redox) state and pH exert a strong influence on the speciation of dissolved components and the solubility of minerals in hydrothermal fluids. log f_{O_2}–pH diagrams were used to depict the influence of oxygen fugacity and pH on monocarboxylate- and dicarboxylate-transport of Pb and Zn in low-temperature (100 °C) hydrothermal ore fluids that are related to diagenetic processes in deep sedimentary basins, and allow a first-order comparison of Pb and Zn transport among proposed model fluids for Mississippi Valley-type (MVT) and red-bed related base metal (RBRBM) deposits in terms of their approximate pH and f_{O_2}conditions. To construct these diagrams, total Pb and Zn concentrations and Pb and Zn speciation were calculated as a function of log f_{O_2} and pH for a composite ore-brine with concentrations of major elements, total sulfur, and total carbonate that approximate the composition of MVT and RBRBM model ore fluids and modern basinal brines. In addition to acetate and malonate complexation, complexes involving the ligands Cl^-, HS^-, H_2S, and OH^- were included in the model of calculated total metal concentration and metal speciation. Also, in the model, Zn and Pb are competing with the common-rock forming metals Ca, Mg, Na, Fe, and Al for the same ligands. Calculated total Pb concentration and calculated total Zn concentration are constrained by galena and sphalerite solubility, respectively. Isopleths, in log f_{O_2}–pH space, of the concentration of Pb and concentration of Zn in carboxylate (acetate + malonate) complexes illustrate that the oxidized model fluids of T. H. Giordano (in *Organic Acids in Geological Processes*, ed. E. D. Pittman and M. D. Lewan, Springer-Verlag, New York, 1994, pp. 319–354) and G. M. Anderson (*Econ. Geol.*, 1975, **70**, 937–942) are capable of transporting sufficient amounts of Pb (up to 10 ppm) and Zn (up to 100 ppm) in the form of carboxylate complexes to form economic deposits of these metals. On the other hand, the reduced ore fluid models of D. A. Sverjensky (*Econ. Geol.*, 1984, **79**, 23–37) and T. H. Giordano and H. L. Barnes (*Econ. Geol.*, 1981, **76**, 2200–2211) can at best transport amounts of Pb and Zn, as carboxylate complexes, that are many orders of magnitude below the 1 to 10 ppm minimum required to form economic deposits. Lead and zinc speciation (mol% of total Pb or Zn) in the model ore fluid was calculated at specific log f_{O_2}–pH conditions along the 100, 0.01, and 0.001 ppm total Pb and total Zn isopleths. Along the 100 ppm isopleth conditions are oxidized ($\Sigma SO_4 \gg \Sigma H_2S$) with Pb and Zn predominantly in the form of chloride complexes under acid to mildly alkaline conditions (pH from 3 to approximately 7.5), while hydroxide complexes dominate Pb and Zn speciation under more alkaline conditions. Sulfide complexes are insignificant under these oxidized conditions. For more reduced conditions along the 0.01 and 0.001 ppm isopleths chloride complexes dominate Pb and Zn speciation in the SO_4^{2-} field and near the SO_4^{2-}–reduced sulfur boundary from pH = 4 to approximately 7.5, while hydroxide complexes dominate Pb and Zn speciation under alkaline conditions above pH = 7.5 in the SO_4^{2-} field. In the most reduced fluids ($\Sigma H_2S \gg \Sigma SO_4$) along the 0.01 and 0.001 isopleths, sulfide complexes account for almost 100% of the Pb and Zn in the model fluid. Acetate (monocarboxylate) complexation is significant only under conditions of chloride and hydroxide complex dominance and its effect is maximized in the pH range 5 to 7, where it complexes 2 to 2.6% of the total Pb and 1 to 1.25% of the total Zn. Malonate (dicarboxylate) complexes are insignificant along all isopleths. The speciation results from this study show that deep formation waters characterized by temperatures near 100 °C, high oxidation states and $\Sigma H_2S < 0.03$ mg L^{-1} ($\Sigma m_{H_2S} < 10^{-6}$), high chlorinities ($\sim$100 000 mg L^{-1}), and high but reasonable concentrations of carboxylate anions can mobilize up to 3% of the total Pb and up to 1.3% of the total Zn as carboxylate complexes. Furthermore, these percentages, under the most favorable conditions, correspond to approximately 1 to 100 ppm of these metals in solution; concentrations that are adequate to form economic deposits of these metals. However, the field evidence suggests that all of these optimum conditions for carboxylate complexation are rarely met at the same time. A comparison of the composite ore fluid compositions from this study and modern brine data shows that the ore brines, corresponding to log f_{O_2}–pH conditions based on the Anderson (1975) and Giordano (1994) model fluids, are similar in many respects to modern, high trace-metal petroleum-field brines. The principal differences between modern high trace-metal brines and the composite ore fluids of Anderson (1975) and Giordano (1994) relate to their carboxylate anion content. The reported concentrations of monocarboxylate anions (Σmonocbx) and dicarboxylate anions (Σdicbx) in high trace-metal petroleum-field brines (<1 to 300 mg L^{-1} and < 1 mg L^{-1}, respectively) are significantly lower than the concentrations assumed in the modelled brines of this study

 DOI: 10.1039/b204459e

(Σmonocbx = 7 700 mg L^{-1} and Σdicbx = 300 mg L^{-1}). There are also major differences in the corresponding total chloride to carboxylate ratio ($\Sigma m_{Cl}/\Sigma m_{cbx}$) and monocarboxylate to dicarboxylate ratio ($\Sigma m_{monocbx}/\Sigma m_{dicbx}$). Modern high trace-metal brines have much higher $\Sigma m_{Cl}/\Sigma m_{cbx}$ values and, therefore, the contribution of carboxylate complexes to the total Pb and Zn content in these modern brines is likely to be significantly less than the 1 to 3 percent for the composite ore fluids of Anderson (1975) and Giordano (1994). The composite ore-brine based on the Giordano and Barnes (1981) MVT ore fluid is comparable to the high salinity (>170 000 mg L^{-1} TDS) subset of modern brines characterized by low trace-metal content and high total reduced sulfur (ΣH_2S). A comparison of the Sverjensky (1984) composite ore-brine with modern petroleum-field brines in terms of ΣH_2S and Zn content, reveals that this ore fluid corresponds to a "border-type" brine, between modern high trace-metal brines and those with low trace-metal content and high ΣH_2S. A brine of this type is characterized by values of ΣH_2S, ΣZn, and/or ΣPb within or near the 1 to 10 mg L^{-1} range. Based on brine-composition data from numerous references cited in this paper, border-type brines do exist but are rare. The model results and field evidence presented in this study are consistent with other chemical simulation studies of carboxylate complexation in modern petroleum-field brines. Thus, it appears that carboxylate complexation plays a minor, if not insignificant, role as a transport mechanism for Pb and Zn in high salinity Na–Cl and Na–Ca–Cl basinal brines and related ore fluids.

Introduction

It is well established through field observations, experiments, and chemical models that oxidation (redox) state and pH exert a strong influence on the speciation of dissolved components and the solubility of minerals in hydrothermal fluids. These parameters are also known to act as major constraints on the stability of specific minerals and mineral assemblages in hydrothermal systems and to control sulfur and carbon isotope systematics in these systems. Of particular interest to this study is the influence of pH and redox state on the speciation of metals, ligands, and metal complexes. For example, in the model presented below, zinc monoacetate complexation, as represented by the reaction

$$Zn^{2+} + CH_3COO^- \rightarrow Zn(CH_3COO)^+$$

is directly influenced by pH through the control of acetate activity by protonation,

$$\underset{\text{(acetate)}}{CH_3COO^-} + H^+ \rightarrow \underset{\text{(acetic acid)}}{CH_3COOH}$$

and the control of Zn^{2+} activity by sphalerite solubility,

$$\underset{\text{(sphalerite)}}{ZnS(s)} + H^+ \rightarrow Zn^{2+} + HS^-$$

The oxygen fugacity indirectly affects reaction (1) because HS^- in reaction (3) is constrained, assuming constant total dissolved sulfur, constant pH and equilibrium, by the SO_4^{2-} to HS^- ratio of the fluid through the reaction,

$$HS^- + 2O_2(g) \rightarrow SO_4^{2-} + H^+$$

and corresponding mass action condition at equilibrium:

$$K = \frac{[SO_4][H^+]}{[HS^-]f^2_{o_2(g)}}$$

In eqn. (5), the bracketed species represent the activity of the enclosed species and f_{O_2} is the fugacity of oxygen gas in equilibrium with the fluid. It has been suggested (*cf.* Shock,[1–3] Helgeson *et al.*[4]) that dissolved acetate is coupled to dissolved carbonate in basinal fluids *via* metastable redox equilibria including the oxidation of acetate by molecular oxygen,

$$CH_3COO^- + 2O_2(g) \rightarrow 2HCO_3^- + H^+$$

This type of metastable link between carboxylate species and carbonate is not assumed in the model described below. In this model total acetate and total malonate concentrations are independent of total carbonate.

Oxygen fugacity (or activity) is the most commonly used redox variable for describing the oxidation state of hydrothermal systems. Its common use stems from the convenience of writing many hydrothermal reactions in terms of oxygen gas as a reactant or product and the generally close approach to (or actual attainment of) stable or metastable equilibrium under hydrothermal conditions. Consequently, $\log f_{O_2}$–pH (or $\log a_{O_2}$–pH) diagrams have become the most widely used approach to illustrate the combined effects of pH and redox state in the control of hydrothermal aqueous speciation and related phase equilibria (Barnes and Kullerud,[5] Barnes and Czamanske,[6] Ripley and Ohmoto,[7] Henley *et al.*,[8] McPhail,[9] Wood[10]). These diagrams can also be employed to graphically represent aqueous carbon and sulfur isotope systematics (Ohmoto,[11] Ohmoto and Rye,[12] Zhang[13]) and organic matter composition (Helgeson *et al.*,[4] Gize[14]) under hydrothermal conditions. In addition to $\log f_{O_2}$–pH diagrams, other graphical depictions of hydrothermal redox dependency are used, including: (a) plots in $\log (\Sigma SO_4/\Sigma H_2S)$–pH and $\log (\Sigma SO_4/\Sigma H_2S)$–$T$ space (Ripley and Ohmoto,[7,15] Ahmad *et al.*,[16] Ohmoto and Goldhaber[17]), (b) $\log f_{S_2}$–T and $\log f_{S_2}$–$1/T$ diagrams (Ripley and Ohmoto,[15] Ohmoto *et al.*,[18] Henley *et al.*[8]), (c) $\log f_{O_2}$–T, $\log f_{O_2}$– $1/T$, and $\log(f_{H_2O}/f_{H_2})$–T diagrams (Ripley and Ohmoto,[7] Ohmoto and Rye,[12] Eugster,[19] Helgeson *et al.*,[4] Ohmoto and Goldhaber,[17] Giggenbach,[20] Cooke *et al.*,[21] Wood and Samson[22]), (d) plots in Eh (pe)–pH space (Rose,[23,24] Wintsch,[25] Henley *et al.*,[8] Pound *et al.*,[26] Pourbaix and Pourbaix[27]), (e) $\log f_{H_2}$–T diagrams (Shock[3]), and (f) the activity diagrams $\log a_i$– $\log a_{CO_2}$ (Helgeson *et al.*[4]), $\log f_{O_2}$– $\log a_{H_2S}$ (Kettler *et al.*[28]), $\log a_{SO_4}$–$\log a_{H_2S}$ (Ohmoto *et al.*[18]), and $\log f_{O_2}$– $\log f_{S_2}$ (Barton *et al.*,[29] Casadevall and Ohmoto,[30] Ohmoto *et al.*,[18] Henley *et al.*,[8] Eugster,[19] Sverjensky,[31,32] Ahmad *et al.*[16]).

Over the past forty years these diagrams, particularly $\log f_{O_2}$–pH diagrams, have been used to investigate transport and deposition mechanism of metals in hydrothermal ore fluids. In the majority of these studies, the principal focus is on inorganic complexation mechanisms that mobilize metals in solution and associated processes that cause complex destabilization and concomitant ore deposition. Although a large number of inorganic ligands are known to be complexing agents in hydrothermal ore fluids, inorganic transport of Hg, Pb, Zn, Cu, REE, and the precious metals appears to be dominated by the ligands Cl^-, HS^-, NH_3, and OH^- (Seward and Barnes[33]). Thus, it is not surprising, that ore transport and deposition processes have been commonly evaluated using concentration contours of metal complexes involving these ligands in $\log f_{O_2}$–pH space. This approach has been particularly fruitful in developing or evaluating genetic models for a wide variety of hydrothermal deposit-types, including mercury deposits (Wells and Ghiorso,[34] Barnes and Seward,[35] Fein and Williams-Jones[36]), Mississippi Valley-type (MVT) deposits (Anderson,[37,38]

Giordano and Barnes,[39] Barnes,[40] Sverjensky[41]), red-bed related base metal (RBRBM) deposits (Sverjensky[31,32]), McArthur-type and Selwyn-type sedex deposits (Cooke *et al.*[21]), porphyry copper deposits (Crerar and Barnes[42]), gold and silver deposits (Barton *et al.*,[29] Casadevall and Ohmoto,[30] Ahmad *et al.*,[16] Gammons and Williams-Jones[43]), as well as deposits of the more exotic metals including the platinum group elements (Mountain and Wood,[44] Wood *et al.*,[45] Gammons *et al.*[46]).

Although inorganic transport mechanisms adequately account for the genesis of many medium- and high-temperature hydrothermal deposits (*e.g.*, porphyry Cu–Mo–W deposits; skarn deposits; and epithermal base metal, Hg, Au, and Ag deposits) it is less certain that such mechanisms can fully account for most lower-temperature hydrothermal deposits formed in the 50 to 200 °C temperature range, especially those deposits intimately associated with organic matter and formed by basinal diagenetic processes (*e.g.*, MVT and RBRBM deposits). As a means of addressing metal transport in these lower-temperature hydrothermal ore systems, alternative complexing mechanisms have been tested including organic transport, involving transport of metals *via* organic ligands in the form of metal-organic complexes (*cf.* Giordano and Barnes,[39] Giordano,[47] Drummond and Palmer,[48] Manning,[49] Hennet *et al.*,[50] Giordano and Kharaka,[51] Sicree and Barnes,[52] Giordano[53]) and *via* pressure-sensitive species such as metal-thiocarbonate complexes (Hennet *et al.*[54]). Furthermore, many epithermal precious metal and mercury deposits contain organic matter with paragenetic relationships closely related to the timing of ore-formation. This observation has sparked speculation that a significant role for organic complexing may supplement or dominate apparently viable inorganic mechanisms of metal transport in these systems (*cf.* Fein and Williams-Jones,[36] Leventhal and Giordano[55]).

Giordano[53] gives an overview of those investigations conducted during the past 25 years and designed to evaluate organic transport in hydrothermal ore systems. The majority of these investigations (experimental and theoretical) have focused on Pb and Zn transport in MVT and RBRBM deposits and deep sedimentary basin brines, generally thought to be ore fluids for these deposits. In all of these studies Pb and Zn concentrations and speciation are either measured or calculated for very restricted fluid compositions in terms of f_{O_2}, pH, and other solute activities. This approach is fine for evaluating the significance of complexing mechanisms under specific ore-fluid conditions. More useful, however, would be an evaluation based on metal concentration contours in log f_{O_2}–pH space. This is the method employed in those studies mentioned above in which log f_{O_2}–pH diagrams were used to develop transport and deposition models based on inorganic complexing. This approach allows a broad-based evaluation of a particular complexing mechanism over a wider range of possible f_{O_2}–pH conditions and the simultaneous evaluation of deposition processes as a function of f_{O_2} and pH. The author is not aware of any published studies that take this approach in evaluating organic-transport mechanisms of base or precious metals in low- to moderate-temperature hydrothermal ore fluids. However, organic transport of mercury has been evaluated in log f_{O_2}–pH space for hydrothermal ore-forming systems (Wells and Ghiorso,[34] Fein and Williams-Jones[36]). These authors found that methyl mercury as well as acetate and oxalate complexes of mercury do not contribute significantly to Hg transport in the formation of hydrothermal mercury deposits.

The purpose of this paper is to present a preliminary evaluation of the influence of oxygen fugacity and pH on monocarboxylate- and dicarboxylate-transport of Pb and Zn in low-temperature (100 °C) hydrothermal ore fluids that are related to diagenetic processes in deep sedimentary basins. First a description of the chemical model used in this study will be presented. This is followed by a presentation of model results illustrating Pb and Zn solubility and speciation and a discussion of these results in terms of fluid parameters and the compositional characteristics of modern petroleum-field brines. Finally, some conclusions will be presented regarding (a) the similarities between modern petroleum-field brines and ore fluid models of MVT and RBRBM deposits and (b) the systematics of Zn and Pb transport by carboxylate complexation in these basinal brines.

Chemical model

Model ore fluids

Over the past half century, geochemical studies of sedimentary basins, petroleum fields, and ore deposits related to these features have resulted in the general consensus that ore fluids responsible for a wide range of low- to medium-temperature (50 to 200 °C) hydrothermal deposits were in fact Na–Cl/Na–Ca–Cl basinal brines (Beales and Jackson,[56] Carpenter *et al.*,[57] Hitchon,[58] Hanor,[59,60,61,62] Anderson and McQueen,[63] Lyndon,[64] Sverjensky,[31,41] Sangster,[65] Force *et al.*,[66] Heijlen *et al.*[67]). These fluids became enriched in metals as a result of diagenetic processes and migrated from hot, deep basin interiors to more peripheral and structurally active parts of the basin where metals were deposited in host rocks to form a variety of ore deposits ranging from purely epigenetic carbonate-hosted and siliciclastic-hosted deposits to those with a significant sedimentary exhalative component (Bjorlykke and Sangster,[68] Gustafson and Williams,[69] Sangster,[65] Cooke *et al.*[21]). Within this wide range of deposit-types, two important categories of epigenetic ores are carbonate-hosed MVT deposits and RBRBM deposits, base metal ores associated with siliciclastic continental/marginal marine host rocks. Both of these ore-types have been extensively studied in terms of their geology and genesis (*cf.* Kisvarsanyi *et al.*,[70] Sverjensky,[71] Haynes and Bloom,[72] Boyle *et al.*,[73] Leach and Goldhaber,[74] Sicree and Barnes[52]). Detailed ore-fluid models have also been proposed for each of these deposit-types and with respect to the ore fluids in these models, there is general agreement among researchers regarding temperature of transport and deposition, total sulfur and total carbonate concentration, and major element composition. For RBRBM deposits (Rose,[23,24] Sverjensky,[31,32] Branam and Ripley[75]), there is also general agreement that the metal-transporting fluids were oxidized, very low in reduced sulfur (reduced sulfur is here defined as $\Sigma m_{H_2S} = m_{H_2S} + m_{HS^-}$), and slightly acidic. Parameters for a composite RBRBM ore fluid (Giordano[76]) are shown in Table 1 and Fig. 1. Unlike RBRBM deposits, three very different sets of log f_{O_2}–pH conditions have been proposed for MVT ore fluids (Table 1; Fig. 1): (1) reduced and acidic (Sverjensky[41]), (2) reduced and alkaline (Giordano and Barnes[39]), and (3) oxidized/slightly acidic (Anderson[37,38,77]), similar to RBRBM ore fluids and many sulfide-poor petroleum–field brines.

Carboxylate ligands

It is well known that some petroleum-related brines from deep sedimentary basins contain measurable quantities (*x* to *xxx* mg L^{-1}) of base metals (Pb, Zn, Cu) and that many petroleum-field brines contain measurable concentrations (*x* to *xxxx* mg L^{-1}) of discrete, polar organic molecules (particularly carboxylic acid anions) capable of complexing Pb, Zn, and Cu, as well as the more common rock-forming metals mobilized in basinal diagenetic environments. The nature of Pb–Zn rich brines from sedimentary basins will be summarized in the Discussion section of this paper. Lundegard and Kharaka,[78] Giordano and Kharaka,[51] and Kharaka *et al.*[79] summarize the available data concerning the nature and distribution of discrete organic ligands in diagenetic environments. Based on

Table 1 Model ore-fluids for Mississippi Valley-type (MVT) and red-bed related base metal (RBRBM) deposits

Parameter	MVT Anderson[37]	MVT Giordano and Barnes[39]	MVT Sverjensky[41]	RBRBM[a] Giordano[76]	Composite ore-brine (this study)
T/°C	100	100	125	100	100
pH	5.7 to 6.7	6.8 to 7.8	4.5 to 5.5	5.5 to 6.5	variable
log f_{O_2}	−48 to –51	−54 to −58	−50.5 to −51.5	−49 to −51	variable
log Σm_{sulfur}	−2	−2	−4.6	−2	−2
log $\Sigma m_{carbonate}$	−1.37	−2 to −4	−1.52	−2.4	−2
Σm_{Cl^-} (a_{Cl^-})	3.0	(2.0)	2.76 (1.4)	2.0	3.0
Σm_{Na^+} (a_{Na^+})	3.0	(1.5)	1.67 (1.0)	(1.0)	2.81
Σm_{K^+} (a_{K^+})		(0.02)	0.012 (.007)	(0.01)	0.05
$\Sigma m_{Ca^{2+}}$ ($a_{Ca^{2+}}$)	0.1	(0.05)	0.491 (.074)	(0.01)	0.2
$\Sigma m_{Mg^{2+}}$ ($a_{Mg^{2+}}$)		(0.02)	0.056 (0.013)	(0.005)	0.1
Chlorinity[b]	99 530	99 530	93 450	69 050	97 450
Salinity[c]	169 200	169 200	158 865	132 480	179 270
Saturation					
Galena	x	x	x	x	x
Sphalerite	x	x		x	x
Pyrite		x	x		x[d]
Hematite	x			x	x[e]
Magnetite					x[f]
Calcite	x	x		x	
Dolomite			x		
Quartz		x	x	x	x
K-Feldspar		x			x
Muscovite		x			
Kaolinite			x		

[a] The composition of this model ore fluid is a composite based on parameter values proposed by Rose,[23,24] Sverjensky,[31,32] and Branam and Ripley.[75] [b] Chlorinity = Cl^- concentration in mg L^{-1}. Calculated from Σm_{Cl^-} and assuming a fluid density of 1.1g cm^{-3} [c] Salinity = total dissolved solids (TDS) in mg L^{-1}. Calculated assuming a fluid density of 1.1g cm^{-3}. [d] Pyrite stability field only. [e] Hematite stability field only. [f] Magnetite stability field only.

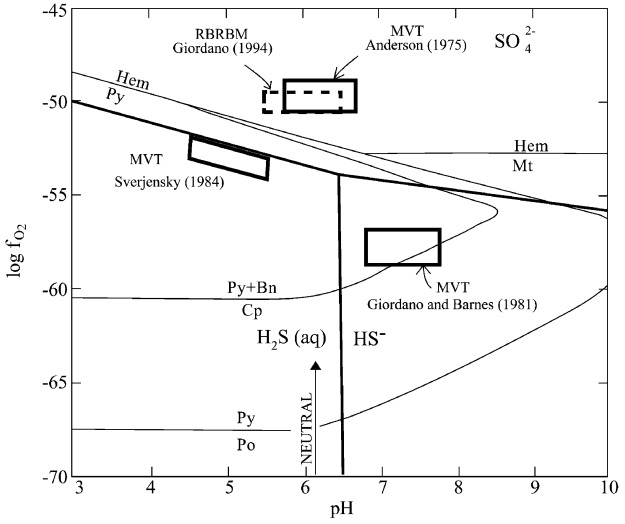

Fig. 1 Approximate log f_{O_2}–pH conditions of Mississippi Valley-type (MVT) and red-bed related base metal (RBRBM) model ore fluids at 100 °C (regions bounded by heavy lines). The stability fields of Cu–Fe–S–O minerals constructed for total sulfur of 10^{-2} mol kg^{-1} and aqueous sulfur species are deliniated by the light and medium boundaries, respectively. Abbreviations: Bn = bornite; Cp = chalcopyrite; Hem = hematite: Mt = magnetite; Po = pyrrhotite; Py = pyrite. Neutral pH is indicated by the vertical arrow.

a critical evaluation of the available analyses of dissolved organic species in petroleum-related brines, these authors conclude that the only clearly identified group of significant organic ligands in oil- and gas-field brines are short-chain aliphatic carboxylate anions. Furthermore, Kharaka *et al.*[79] give recommended maximum concentrations for the most abundant carboxylate anions found in these fluids (Table 2). Acetate is the dominant monocarboxylate anion in brines with temperatures greater than 85 °C followed by propionate, butyrate, and valerate, while the dominant dicarboxylate species are succinate, glutarate, and malonate. Kharaka *et al.*[79] do not rule out the possibility of other important groups of organic ligands but the observational data are not available to support their importance in modern basinal brines and ancient ore fluids. In the model ore fluid evaluated in this paper, acetate with a concentration of 7 700 mg L^{-1} (0.13 *m*) represents the four dominant monocarboxylate ligands and malonate with a concentration of 300 mg L^{-1} (0.0029 *m*) is used to represent the three dominant dicarboxylate ligands (Table 2). This approach was taken because there is a lack of experimental thermodynamic data for complexation equilibria involving the ligands propionate, butyrate, valerate, succinate, and glutarate. Based on experimental data at 25 °C (Smith *et al.*[80]) and predicted constants at elevated temperatures (Shock and Koretsky,[81] Sverjensky *et al.*,[82] Prapaipong *et al.*[83]), it appears that malonate, succinate, and glutarate form metal complexes with similar stabilities and that metal acetate complexes are similar in terms of stability to corresponding complexes formed by propionate, butyrate, and valerate. Metal dicarboxylate complexes are generally one to two orders of magnitude stronger than metal monocarboxylate complexes because of the chelate effect. Thus, for a given total carboxylate ligand content, metal carboxylate complexation increases with increasing proportion of dicarboxylate ligand species, or decreasing concentration ratio of total monocarboxylate to total dicarboxylate.

Composite ore fluid

In this paper a composite ore fluid (column 6 in Table 1) is tested for Pb and Zn transport at 100 °C as a function of pH and log f_{O_2}. Concentrations of the major elements, total sulfur, and total carbonate of this hypothetical ore fluid only approximate the proposed concentrations given in columns 2 through 5 of Table 1 for the four model ore-fluids.

Table 2 Most abundant monocarboxylate and dicarboxylate anions observed in petroleum-field brines, their most likely maximum concentration in these fluids, and their concentrations used in the composite ore-fluid model of this study

Acid anion		Petroleum-field brine concentration (likely maximum, mg L^{-1})[a]	Model ore-fluid concentration	
IUPAC	Common		/mg L^{-1}	/mol kg^{-1}
Monocarboxylate anions				
Ethanoate	Acetate	5000	7700	0.13
Propanoate	Propionate	2000	—	—
Butanoate	Butyrate	500	—	—
pentanoate	Valerate	200	—	—
Dicarboxylate anions				
Propanedioate	Malonate	100	300	0.0029
Butanedioate	Succinate	100	—	—
Pentanedioate	Glutarate	100	—	—

[a] Kharaka *et al.*[79]

Table 3 Equilibrium constants for acetate and malonate complexes of Pb and Zn used in model calculations

Acetate ($Ac^- = CH_3COO^-$)				Malonate ($Ma^{2-} = C_3H_2O_4^{2-}$)			
Reaction	Log K	T/°C	Ref.[a]	Reaction	Log K	T/°C	Ref.[a]
$H^+ + Ac^- \rightarrow Hac$	4.94	100	1	$H^+ + HMa^- \rightarrow H_2Ma$	3.02	100	5
				$H^+ + Ma^{2-} \rightarrow HMa^-$	6.14	100	5
$Pb^{2+} + Ac^- \rightarrow PbAc^+$	3.00	100	2				
$Pb^{2+} + 2Ac^- \rightarrow Pb(Ac)_2$	4.69	100	2	$Pb^{2+} + Ma^{2+} \rightarrow PbMa$	2.79	25	6
$Pb^{2+} + 3Ac^- \rightarrow Pb(Ac)_3^-$	3.66	100	3	$Pb^{2+} + 2Ma^{2+} \rightarrow Pb(Ma)_2^{2-}$	5.70	25	6
				$Pb^{2+} + HMa^- \rightarrow PbHMa^+$	2.40	25	6
$Zn^{2+} + Ac^- \rightarrow ZnAc^+$	2.30	100	4	$Pb^{2+} + 2HMa^- \rightarrow Pb(HMa)_2$	2.40	25	6
$Zn^{2+} + 2Ac^- \rightarrow Zn(Ac)_2$	4.00	100	4				
$Zn^{2+} + 3Ac^- \rightarrow Zn(Ac)_3^-$	4.70	100	4	$Zn^{2+} + Ma^{2-} \rightarrow ZnMa$	3.84	25	7
				$Zn^{2+} + 2Ma^{2-} \rightarrow Zn(Ma)_2^{2-}$	5.40	25	7
				$Zn^{2+} + HMa^+ \rightarrow ZnHMa^+$	1.00	25	7

[a] (1) Mesmer *et al.*[84] (2) Extrapolation based on 24 to 85 °C data from Giordano[85] and Hennet *et al.*[50] (3) SOLMINEQ.88, Kharaka *et al.*[86] (4) Giordano and Drummond.[87] (5) Kettler *et al.*[88] (6) Data from Hammam *et al.*[89] extrapolated to $I = 0$. (7) Evans and Monk.[90]

Nevertheless, the concentrations of the major elements, total carbonate, and total sulfur of this composite ore fluid are sufficiently close to those of the other model fluids, as well as many petroleum-field brines, to allow a first-order comparison of Pb and Zn transport among the proposed model fluids in terms of their approximate pH and f_{O_2}conditions. The primary purpose of this paper is to evaluate the influence of these two parameters on Zn and Pb transport by monocarboxylate ligands represented by acetate complexation and dicarboxylate ligands represented by malonate complexation. The stability constants used in this study to describe malonate and acetate protonation and malonate and acetate complexation of Pb and Zn are given in Table 3. Reliable 100 °C constants are available for the protonation equilibria and acetate complexation of Pb and Zn. However, the author is not aware of reliable 100 °C data for malonate complexation of Pb and Zn and, therefore, the available 25 °C data are used. Although thermodynamic data are available for Cu^+–acetate complexes between 50 and 150 °C (Liu *et al.*[91]), the lack of thermodynamic data for Cu^+–dicarboxylate complexes (Martell and Smith,[92,93] Smith and Martell,[94] Smith *et al.*[80]) precluded the possibility of adequately modeling Cu complexation in this study. It should be noted that Sverjensky's1984 model MVT-fluid[41] has a temperature of 125 °C and, therefore, the log $f_{O_2}$and pH boundaries defined by Sverjensky[41] were used in this study to estimate correlative log $f_{O_2}$and pH boundaries at 100 °C (Fig. 1 and Table 1).

Total Pb and Zn concentrations and Pb and Zn speciation were calculated as a function of log f_{O_2} and pH for the composite ore-brine described in Table 1. In addition to acetate and malonate complexation, complexes involving the ligands Cl^-, HS^-, H_2S, and OH^- were included in the model of calculated total metal concentration and metal speciation. Also, in the model calculations, Zn and Pb are competing with the common-rock forming metals Ca, Mg, Na, Fe, and Al for the same ligands. Calculated total Pb concentration and calculated total Zn concentration are constrained by galena and sphalerite solubility, respectively. It was assumed that the brine is saturated with respect to quartz and K-feldspar at all log f_{O_2}–pH conditions and that total Fe concentration is controlled by either pyrite, hematite or magnetite solubility, depending on the given f_{O_2}–pH condition. The stability fields for pyrite, hematite, and magnetite are shown in Fig. 1. K-Feldspar is the stable aluminum phase throughout only part of the log f_{O_2}–pH conditions represented in Fig. 1. Because the calculated Pb and Zn values are not significantly affected by Al speciation, the assumption of K-feldspar saturation has little influence on Pb and Zn solubility in this model. The model does not constrain the activities of Ca^{2+} and Mg^{2+} by calcite or dolomite solubility. Although these cations affect the speciation of carboxylate ligands, their overall influence on Pb and Zn speciation, in the model, is negligible. Pb and Zn isopleths in log f_{O_2}–pH space are presented in Fig. 2 through 5, while speciation of Pb and Zn along specific isopleths is presented in Tables 4 through 9 and Fig. 6 through 11.

Results

Isopleths

It is generally assumed that an ore fluid must transport, at a minimum, between 1 and 10 ppm of a base metal to form an ore deposit of that metal (Barnes and Czamanske,[6] Barnes,[40,95] Anderson,[38] Roedder,[96] Ohmoto,[97] Seward and Barnes[33]). Examination of the Pb isopleths (representing galena solubility) in Fig. 2 shows that sufficient lead in the model ore fluid can only be transported under log f_{O_2}–pH conditions corresponding to low total sulfide ($\Sigma m_{SO_4} \gg \Sigma m_{H_2S}$); for example, the relatively oxidized RBRBM ore fluid of Giordano[76] and the MVT ore fluid of Anderson.[37] The MVT ore fluids of Sverjensky[41] and Giordano and Barnes[39] are capable of

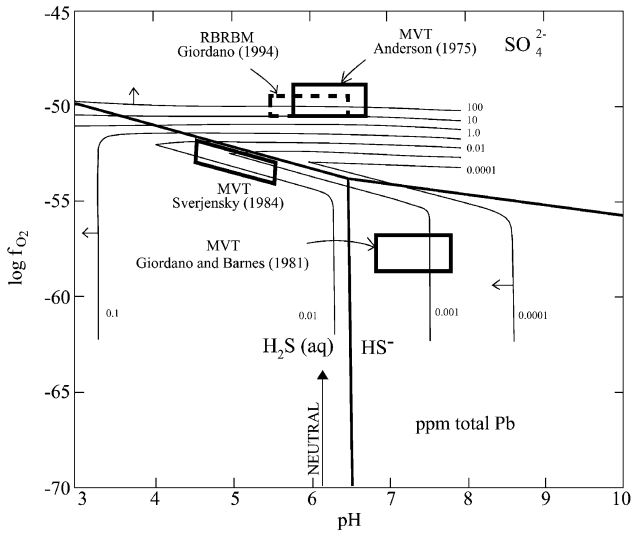

Fig. 2 Total ppm Pb isopleths in log f_{O_2}–pH space for the model composite ore-brine at 100 °C. Neutral pH, log f_{O_2}–pH conditions for the model ore fluids, regions of mineral stability, and regions of dominance for sulfur species are the same as illustrated in Fig. 1. The small arrows indicate the direction of increasing concentration.

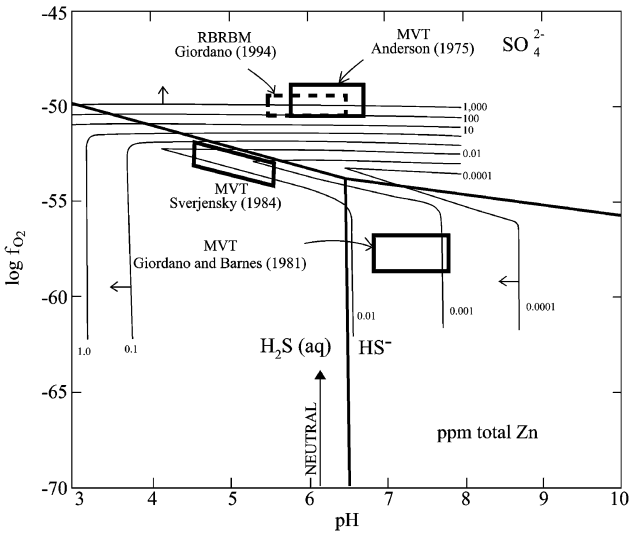

Fig. 3 Total ppm Zn isopleths in log f_{O_2}–pH space for the model composite ore-brine at 100 °C. Neutral pH, log f_{O_2}–pH conditions for the model ore fluids, regions of mineral stability, and regions of dominance for sulfur species are the same as illustrated in Fig. 1. The small arrows indicate the direction of increasing concentration.

transporting maximum amounts of lead that are 2 to 5 orders of magnitude below the 1 to 10 ppm minimum. It should be noted that Sverjensky's 1984 model ore fluid[41] was developed for a temperature of 125 °C and that the model fluid could barely transport 1ppm Pb at that temperature. The total Zn isopleths (representing sphalerite solubility) shown in Fig. 3 illustrate model results similar to those for Pb. The ore fluids of Sverjensky[41] and Giordano and Barnes[39] are not capable of transporting sufficient Zn at 100 °C. However, the oxidized RBRBM ore fluid of Giordano[76] and the Anderson MVT ore fluid can clearly mobilize 100s of ppm Zn, several orders of magnitude greater than the minimum required to form economic deposits of Zn.

In Fig. 4 and 5, respectively, isopleths of the total concentration of Pb and total concentration of Zn in carboxylate (acetate + malonate) complexes are plotted for the model ore fluid. The 1 to 10 ppm Pb isopleths shown in Fig. 4 illustrate that the oxidized model fluids of Giordano[76] and Anderson[37] are capable of transporting sufficient amounts of Pb in the form of carboxylate complexes to form economic deposits of lead. On the other hand, the reduced ore fluid models of Sverjensky[41] and Giordano and Barnes[39] can at best transport amounts of Pb, as carboxylate complexes, that are many orders of magnitude below the 1 to 10 ppm minimum. Similar to Pb, the 1 and 10 ppm Zn isopleths in Fig. 5 coincide with the log f_{O_2}–pH conditions of the RBRBM and Anderson MVT ore fluids and demonstrate that these brines can transport sufficient Zn, as carboxylate complexes at 100 °C, to form economic deposits of Zn. However, the more reduced Sverjensky[41] and Giordano and Barnes[39] ore fluids are incapable of transporting sufficient Zn, as carboxylate complexes, to form economically

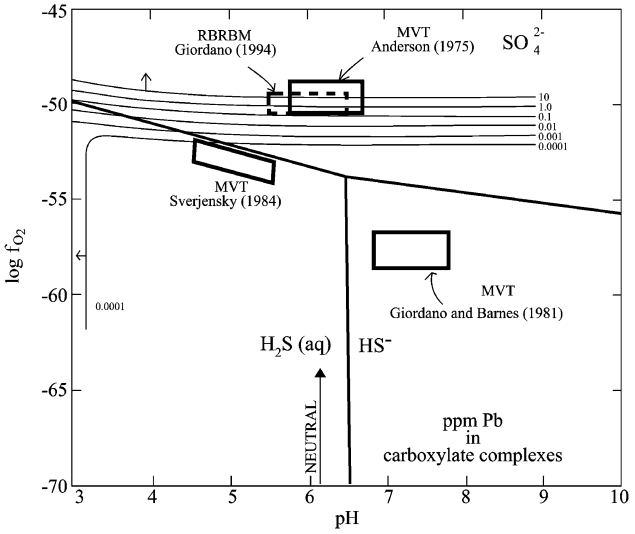

Fig. 4 Isopleths of total ppm Pb in carboxylate complexes as a function of log $f_{O_2}$and pH for the model composite ore-brine. Neutral pH, log f_{O_2}–pH conditions for model ore fluids, regions of mineral stability, and regions of dominance for sulfur species are the same as illustrated in Fig. 1. The small arrows indicated the direction of increasing concentration.

viable deposits of Zn. The isopleths in Fig. 4 and 5 curve upward on the left side of the diagram because protonation of acetate and malonate becomes significant at pH below 5, thereby reducing the activities of these ligands in solution and

Table 4 Lead speciation, as a function of pH and log f_{O_2} along the 100 ppm Pb isopleth of the model composite ore-brine at 100 °C[ab]

pH	Log f_{O_2}	Iron phase[c] saturation	Cation	Chloride complexes	Sulfide complexes	Hydroxide complexes	Acetate complexes	Malonate complexes	Data set
8.00	−50.20	Hm	0.06	23.60	2.3×10^{-14}	74.47	0.80	2.6×10^{-3}	5
7.00	−49.95	Hm	0.17	72.64	6.9×10^{-13}	22.38	2.59	8.3×10^{-3}	4
5.00	−49.90	Hm	0.23	97.25	5.9×10^{-9}	0.30	2.19	9.9×10^{-3}	3
4.00	−49.90	Py	0.24	99.21	6.0×10^{-7}	0.03	0.51	8.9×10^{-3}	2
3.00	−49.90	Py	0.24	99.69	6.0×10^{-5}	3.2×10^{-3}	0.05	6.3×10^{-3}	1

[a] Speciation for the indicated complexes is given as mol% of total Pb. [b] The 100 ppm isopleth is illustrated in Fig. 2. [c] Saturated with respect to hematite (Hm), pyrite (Py), or magnetite (Mt).

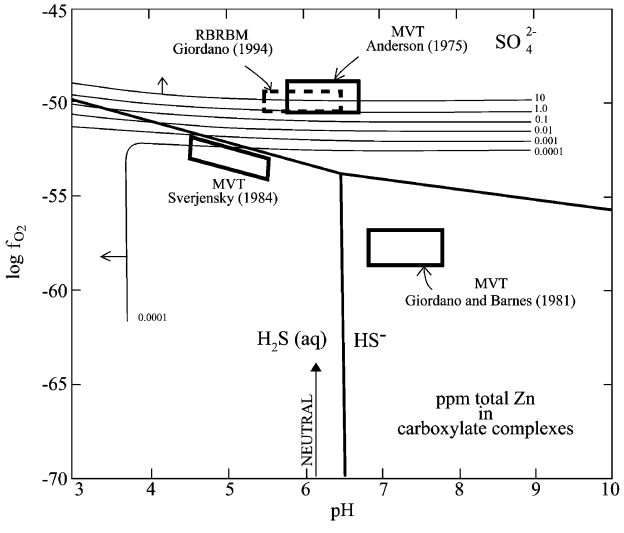

Fig. 5 Isopleths of total ppm Zn in carboxylate complexes as a function of log f_{O_2} and pH for the model composite ore-brine. Neutral pH, log f_{O_2}–pH conditions for model ore fluids, regions of mineral stability, and regions of dominance for sulfur species are the same as illustrated in Fig. 1. The small arrows indicate the direction of increasing concentration.

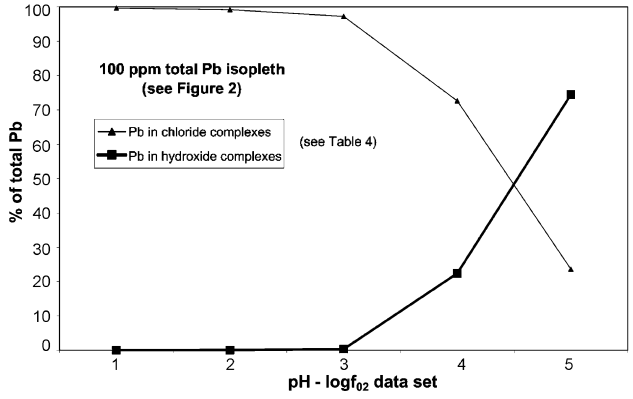

Fig. 6 Percent of total Pb in chloride complexes and hydroxide complexes as a function of pH–log f_{O_2} conditions along the 100 ppm total Pb isopleth in Fig. 2. Specific pH–log f_{O_2} conditions (pH, log f_{O_2}) are given in Table 4, along with corresponding % of total Pb values for various forms of Pb, and begin at the right end of the 100 ppm isopleth with data set #5 (8, −50.20), followed by #4 (7, −49.95), #3 (5, −49.90), #2 (4, −49.90), and #1 (3, −49.90).

the complexation of lead and zinc by them. Under conditions deep within the H_2S field (Fig. 4 and 5) Pb^{2+} and Zn^{2+} activities are constant at a given pH. Therefore, the concentration of individual carboxylate complexes is also constant; thus producing the vertical 0.0001 ppm isopleths in Fig. 4 and 5.

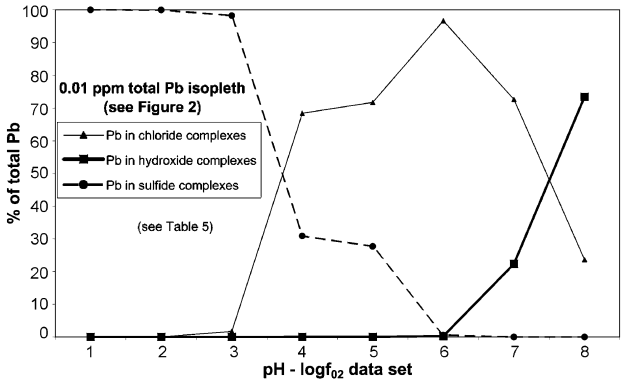

Fig. 7 Percent of total Pb in chloride, hydroxide, and sulfide complexes as a function of pH–log f_{O_2} conditions along the 0.01 ppm total Pb isopleth in Fig. 2. Specific pH–log f_{O_2} conditions (pH, log f_{O_2}) are given in Table 5, along with corresponding % of total Pb values for various forms of Pb, and begin at the right end of the 0.01 ppm isopleth with data set #8 (8, −52.20), followed by #7 (7, −51.95), #6 (5, −51.90), #5 (4, −51.90), #4 (4.2, −52.00), #3 (4.75, −52.90), #2 (5.8, −54.00), and #1 (6.3, −55.00).

Speciation

Lead speciation (mol% of total Pb) in the model ore fluid was calculated at specific log f_{O_2}–pH conditions along the 100, 0.01, and 0.001 ppm total Pb isopleths shown in Fig. 2. These speciation results are presented in Table 4 and Fig. 6, Table 5 and Fig. 7, and Table 6 and Fig. 8 for the 100, 0.01 and 0.001 ppm isopleths, respectively. Along the 100 ppm isopleth (Fig. 2 and 6, Table 4) conditions are oxidized and lead is predominantly in the form of chloride complexes under acid to mildly alkaline conditions (pH from 3 to approximately 7.5), while hydroxide complexes dominate lead speciation under more alkaline conditions (Table 4 and Fig. 6). Sulfide complexes are insignificant under these oxidized conditions. Acetate (monocarboxylate) complexation accounts for up to 2.6% of the total Pb in the pH range 5 to 7, while malonate (dicarboxylate) complexes are insignificant along the isopleth. For the 0.01 ppm isopleth (Fig. 2 and 7, Table 5), chloride complexes dominate lead speciation in the SO_4^{2-} field and near the SO_4^{2-}-reduced sulfur boundary from pH = 4 to approximately 7.5, while hydroxide complexes dominate lead speciation under alkaline conditions above pH = 7.5 in the SO_4^{2-} field. In the most reduced fluids along the 0.01 isopleth, lead sulfide complexes account for almost 100% of the Pb in the model fluid. Acetate (monocarboxylate) complexation is significant only under conditions of chloride and hydroxide complex dominance and its effect is maximized in the pH range 5 to 7, where it complexes 2 to 2.6% of the total Pb. Malonate (dicarboxylate) complexes are insignificant along the 0.01 isopleth. The lead speciation systematics along the 0.001 isopleth (Fig. 2 and 8, Table 6) are similar to those for the 0.01

Table 5 Lead speciation, as a function of pH and log f_{O_2} along the 0.01 ppm Pb isopleth of the model composite ore-brine at 100 °C[ab]

pH	Log f_{O_2}	Iron phase[c] saturation	Cation	Chloride complexes	Sulfide complexes	Hydroxide complexes	Acetate complexes	Malonate complexes	Data set
8.00	−52.20	Hm	5.6×10^{-2}	23.6	2.3×10^{-6}	73.47	0.80	2.6×10^{-3}	8
7.00	−51.95	Hm	0.17	72.64	7.6×10^{-5}	22.37	2.58	8.3×10^{-3}	7
5.00	−51.90	Py	0.23	96.68	0.59	0.30	2.18	0.01	6
4.00	−51.90	Py	0.17	71.75	27.67	0.02	0.37	6.4×10^{-3}	5
4.20	−52.00	Py	0.17	68.42	30.85	0.03	0.52	6.3×10^{-3}	4
4.75	−52.90	Py	4.1×10^{-3}	1.70	98.26	3.0×10^{-3}	0.03	1.7×10^{-4}	3
5.80	−54.00	Py	3.5×10^{-5}	0.02	99.98	2.9×10^{-4}	4.6×10^{-4}	1.6×10^{-6}	2
6.30	−55.00	Py	3.2×10^{-6}	1.4×10^{-3}	99.99	8.4×10^{-5}	4.6×10^{-5}	1.5×10^{-7}	1

[a] Speciation for the indicated complexes is given as mol% of total Pb. [b] The 0.01 ppm isopleth is illustrated in Fig. 2. [c] Saturation with respect to hematite (Hm), pyrite (Py), and magnetite (Mt).

Table 6 Lead speciation, as a function of pH and log f_{O_2} along the 0.001 ppm Pb isopleth of the model composite ore-brine at 100 °C[ab]

pH	Log f_{O_2}	Iron phase[c] saturation	Cation	Chloride complexes	Sulfide complexes	Hydroxide complexes	Acetate complexes	Malonate complexes	Data set
8.00	−52.70	Hm	0.06	23.60	2.3×10^{-4}	73.47	0.80	2.6×10^{-3}	7
6.00	−52.40	Py	0.22	93.09	0.57	2.89	3.04	0.01	6
6.00	−53.55	Py	1.1×10^{-3}	0.48	99.49	0.02	0.02	5.2×10^{-5}	5
6.45	−54.00	Py	1.6×10^{-4}	0.07	99.92	5.8×10^{-3}	2.3×10^{-3}	7.5×10^{-6}	4
7.00	−54.60	Py	1.3×10^{-5}	5.4×10^{-3}	99.99	1.7×10^{-3}	1.9×10^{-4}	6.1×10^{-7}	3
7.30	−55.00	Py	3.2×10^{-6}	1.3×10^{-3}	99.99	8.3×10^{-4}	4.7×10^{-5}	1.5×10^{-7}	2
7.55	−57.00	Py	9.4×10^{-7}	3.9×10^{-4}	99.99	4.3×10^{-4}	1.3×10^{-5}	4.3×10^{-8}	1

[a] Speciation for the indicated complexes is given as mol% of total Pb. [b] The 0.001 ppm isopleth is illustrated in Fig. 2. [c] Saturation with respect to hematite (Hm), pyrite (Py), or magnetite (Mt).

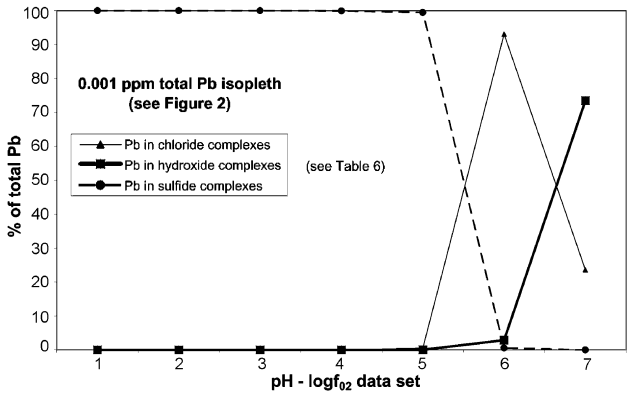

Fig. 8 Percent of total Pb in chloride, hydroxide, and sulfide complexes as a function of pH–log f_{O_2} conditions along the 0.001 ppm total Pb isopleth in Fig. 2. Specific pH–log f_{O_2} conditions (pH, log f_{O_2}) are given in Table 6, along with corresponding % of total Pb values for various forms of Pb, and begin at the right end of the 0.001 ppm isopleth with data set #7 (8, −52.70), followed by #6 (6, −52.40), #5 (6, −53.55), #4 (6.45, −54.00), #3 (7, −54.60), #2 (7.3, −55.00), and #1 (7.55, −57.00).

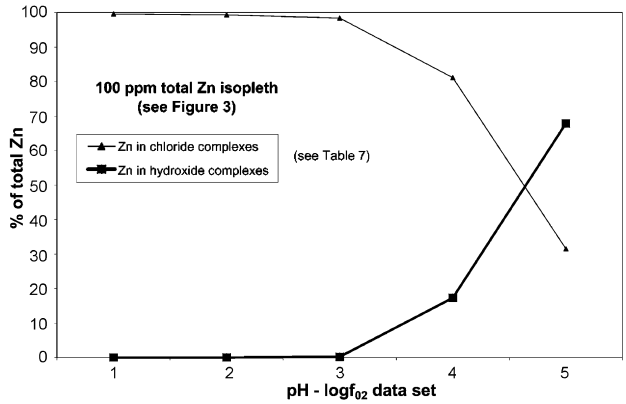

Fig. 9 Percent of total Zn in chloride complexes and hydroxide complexes as a function of pH–log f_{O_2} conditions along the 100 ppm total Zn isopleth in Fig. 3. Specific pH–log f_{O_2} conditions (pH, log f_{O_2}) are given in Table 7, along with corresponding % of total Zn values for various forms of Zn, and begin at the right end of the 100 ppm isopleth with data set #5 (8, −50.55), followed by #4 (7, −50.35), #3 (5, −50.30), #2 (4, −50.30), and #1 (3, −50.30).

isopleth. Chloride and hydroxide complexation dominate the speciation of Pb in the SO_4^{2-} field and near the SO_4^{2-}-reduced sulfur boundary, while sulfide complexes account for most of the Pb under reduced conditions below the SO_4^{2-}-reduced sulfur boundary. Acetate (monocarboxylate) complexes comprise a significant portion of the Pb (up to 3%) in oxidized, weakly acid to mildly alkaline (6 to 8 pH range) fluids, while malonate (dicarboxylate) complexes are insignificant under all conditions along the 0.001 isopleth.

The speciation systematics for Zn in the model fluid are, in general, similar to those for Pb. Zinc speciation (mol% of total Zn) in the model ore fluid was calculated at specific log f_{O_2}–pH conditions along the 100, 0.01, and 0.001 ppm total Zn isopleths shown in Fig. 3. These speciation results are presented in Table 7 and Fig. 9, Table 8 and Fig. 10, and Table 9 and Fig. 11 for the 100, 0.01, and 0.001 ppm isopleths, respectively. Along the 100 ppm isopleth (Fig. 3 and 9, Table 7) conditions are oxidized and chloride complexation dominates the speciation of Zn in acid to mildly alkaline conditions (pH from 3 to approximately 7.5), while hydroxide complexation dominates zinc speciation under pHs ranging from approximately 7.5 into the alkaline region. Sulfide complexes are insignificant under these oxidized conditions. Carboxylate complexation is maximized in the 5 to 7 pH range (where chloride complexation dominates zinc speciation) and is responsible for approximately 1.25% of the total Zn under these conditions. Acetate (monocarboxylate) complexation accounts for approximately 1 to 1.25% of the total Zn, while malonate (dicarboxylate) complexes comprise less than 0.25% of the total Zn under those conditions most favorable for the formation of Zn dicarboxylate complexes. Zinc speciation along the 0.01 ppm (Fig. 3 and 10, Table 8) and 0.001 ppm (Fig. 3 and 11, Table 9) isopleths is similar. For the 0.01 isopleth, hydroxide complexation dominates zinc speciation under oxidized conditions above pHs of approximately 7.5. Zn chloride complexes are predominant in the SO_4^{2-} field and

Table 7 Zinc speciation, as a function of pH and log f_{O_2}along the 100 ppm Zn isopleth of the model composite ore-brine at 100 °C[ab]

pH	Log f_{O_2}	Iron phase[c] saturation	Cation	Chloride complexes	Sulfide complexes	Hydroxide complexes	Acetate complexes	Malonate complexes	Data set
8.00	−50.55	Hm	0.11	31.53	9.2×10^{-14}	67.90	0.45	9.0×10^{-3}	5
7.00	−50.35	Hm	0.28	81.15	3.8×10^{-12}	17.30	1.22	0.02	4
5.00	−50.3	Hm	0.35	98.43	2.9×10^{-8}	0.21	0.97	0.23	3
4.00	−50.3	Py	0.36	99.36	2.9×10^{-6}	0.02	0.24	9.6×10^{-3}	2
3.00	−50.3	Py	0.36	99.60	2.7×10^{-4}	2.2×10^{-3}	0.03	2.0×10^{-3}	1

[a] Speciation for the indicated complexes is given as mol% of total Zn. [b] The 100 ppm isopleth is illustrated in Fig. 3. [c] Saturation with respect to hematite (Hm), pyrite (Py), or magnetite (Mt).

Table 8 Zinc speciation, as a function of pH and log f_{O_2} along the 0.01 ppm Zn isopleth of the model composite ore-brine at 100 °C[ab]

pH	Log f_{O_2}	Iron phase[c] saturation	Cation	Chloride complexes	Sulfide complexes	Hydroxide complexes	Acetate complexes	Malonate complexes	Data set
8.00	−52.55	Hm	0.11	31.53	9.3×10^{-6}	67.90	0.45	9.0×10^{-3}	7
7.00	−52.35	Hm	0.28	81.15	3.8×10^{-4}	17.30	1.22	0.02	6
6.00	−52.30	Py	0.34	96.19	0.03	2.07	1.33	0.03	5
4.75	−52.90	Py	0.04	12.36	87.48	0.02	0.10	2.5×10^{-3}	4
5.78	−54.00	Py	3.9×10^{-4}	0.11	99.89	1.4×10^{-3}	1.5×10^{-3}	3.0×10^{-5}	3
6.40	−55.00	Py	2.4×10^{-5}	6.7×10^{-3}	99.99	3.6×10^{-4}	9.6×10^{-5}	1.9×10^{-6}	2
6.50	−56.00	Py	1.7×10^{-5}	4.8×10^{-3}	99.99	3.2×10^{-4}	6.9×10^{-5}	1.4×10^{-6}	1

[a] Speciation for the indicated complexes is given as mol% of total Zn. [b] The 0.01 ppm isopleth is illustrated in Fig. 3. [c] Saturation with respect to hematite (H), pyrite (Py), or magnetite (Mt).

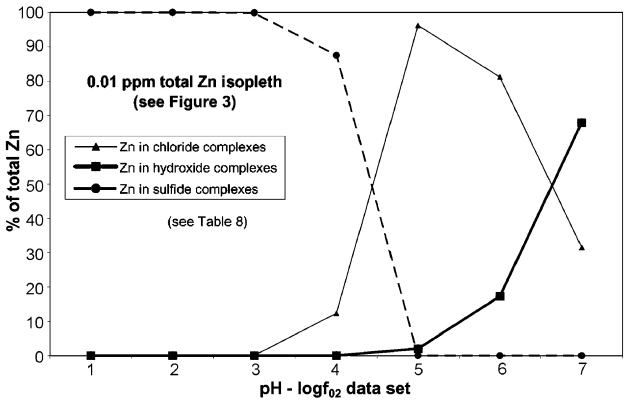

Fig. 10 Percent of total Zn in chloride, hydroxide, and sulfide complexes as a function of pH–log f_{O_2} conditions along the 0.01 ppm total Zn isopleth in Fig. 3. Specific pH–log f_{O_2} conditions (pH, log f_{O_2}) are given in Table 8, along with corresponding % of total Zn values for various forms of Zn, and begin at the right end of the 0.01 ppm isopleth with data set #7 (8, −52.55), followed by #6 (7, −52.35), #5 (6, −52.30), #4 (4.75, −52.90), #3 (5.78, −54.00), #2 (6.4, −55.00), and #1 (6.5, −56.00).

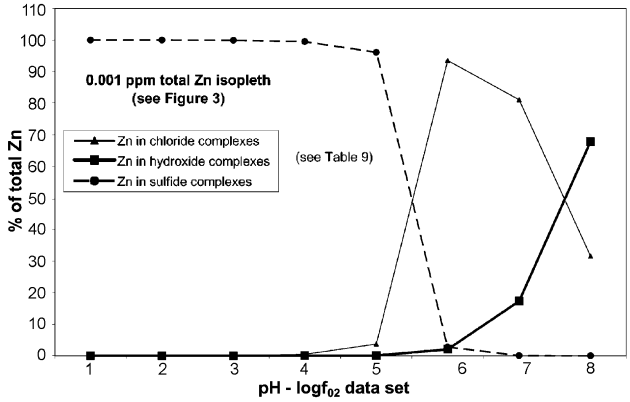

Fig. 11 Percent of total Zn in chloride, hydroxide, and sulfide complexes as a function of pH–log f_{O_2} conditions along the 0.001 ppm total Zn isopleth in Fig. 3. Specific pH–log f_{O_2} conditions (pH, log f_{O_2}) are given in Table 9, along with corresponding % of total Zn values for various forms of Zn, and begin at the right end of the 0.001 ppm isopleth with data set #8 (8, −53.05, followed by #7 (7, −52.85), #6 (6, −52.80), #5 (6, −53.55), #4 (6.4, −54.00), #3 (7, −54.60), #2 (7.3, −55.00), and #1 (7.7, −56.00).

near the SO_4^{2-}-reduced sulfur boundary at pHs ranging from approximately 5 to 7.5, while Zn sulfide complexes account for approximately 87 to near 100% of the total Zn under reduced conditions in the pH range 4.8 to 6.5. Acetate (monocarboxylate) complexation is significant only in oxidized, weakly acid to mildly alkaline solutions and accounts for approximately 1.25 to 1.3% of the total Zn under these conditions. Malonate (dicarboxylate) complexation is maximized, but insignificant, under the same conditions. For the 0.001 isopleth, hydroxide complexation, again, dominates under alkaline conditions in the SO_4^{2-} field and chloride complexes are dominant under acid to mildly alkaline conditions in the SO_4^{2-} field and near the SO_4^{2-}-reduced sulfur boundary, while 90 to nearly 100% of the zinc is complexed by sulfide ligands under reduced conditions below the SO_4^{2-}-reduced sulfur boundary.

Discussion

Percentage of total Pb and Zn in carboxylate complexes: key determinants

The percent of dissolved Zn or Pb complexed by carboxylate ligands in a basinal brine will depend on four key variables, assuming a systems remains invariant with respect to temperature and pressure, total sulfur and total carbonate of the brine, major cation ratios of the brine, and mineralogy of the aquifer. The four variables are (1) the total chloride molality to total carboxylate ligand molality ($\Sigma m_{Cl^-}/\Sigma m_{cbx}$), (2) the mix of specific carboxylate ligands, for example the monocarboxylate to dicarboxylate ratio ($\Sigma m_{monocbx}/\Sigma m_{dicbx}$), (3) the concentration of total inorganic sulfide ($\Sigma m_{H_2S} = m_{H_2S} + m_{HS^-}$), and (4) the pH. Values for these four parameters are

Table 9 Zinc speciation, as a function of pH and log f_{O_2} along the 0.001 ppm Zn isopleth of the model composite ore-brine at 100 °C[ab]

pH	Log f_{O_2}	Iron phase[c] saturation	Cation	Chloride complexes	Sulfide complexes	Hydroxide complexes	Acetate complexes	Malonate complexes	Data set
8.00	−53.05	Mt	0.11	31.53	9.3×10^{-4}	67.90	0.45	9.0×10^{-3}	8
7.00	−52.85	Mt	0.28	81.11	0.04	17.30	1.22	0.02	7
6.00	−52.80	Py	0.33	93.57	2.75	2.01	1.29	0.03	6
6.00	−53.55	Py	0.01	3.73	96.12	0.08	0.05	1.0×10^{-3}	5
6.40	−54.00	Py	1.5×10^{-3}	0.43	99.54	0.02	6.2×10^{-3}	1.3×10^{-4}	4
7.00	−54.60	Py	1.3×10^{-4}	0.04	99.95	7.9×10^{-3}	5.5×10^{-4}	1.1×10^{-5}	3
7.30	−55.00	Py	2.8×10^{-5}	8.0×10^{-3}	99.99	3.4×10^{-3}	1.2×10^{-4}	2.3×10^{-6}	2
7.70	−56.00	Py	6.8×10^{-6}	1.9×10^{-3}	99.99	2.1×10^{-3}	2.8×10^{-5}	5.5×10^{-7}	1

[a] Speciation for the indicated complexes is given as mol% of total Zn. [b] The 0.001 ppm isopleth is illustrated in Fig. 3. [c] Saturation with respect to hematite (H), pyrite (Py), or magnetite (Mt).

Table 10 Comparison of model ore fluids with modern Na–Cl and Na–Ca–Cl basinal brines

Composite ore-brine (this study): log f_{O_2}–pH regions[a]

Parameter	MVT Anderson (1975)[c]	MVT Giordano and Barnes (1981)[d]	MVT Sverjensky (1984)[e]	RBRBM Giordano (1994)[f]
T/°C	100	100	100	100
TDS/mg L^{-1}	179 270	179 270	179 270	179 270
ΣCl^-/mg L^{-1}	97 450	97 450	97 450	97 450
pH	6.0	7.5	4.6	6.0
ΣH_2S/mg L^{-1}[g]	$10^{-6.3}$	340	3.4	$10^{-6.3}$
Σm_{H_2S}[g]	$10^{-10.8}$	10^{-2}	10^{-4}	$10^{-10.8}$
ΣSO_4/mg L^{-1}[h]	960	10^{-2}	960	960
Σm_{SO_4}[h]	10^{-2}	$10^{-7.2}$	10^{-2}	10^{-2}
Σmonocbx/mg L^{-1}[i]	7700	7700	7700	7700
$\Sigma m_{monocbx}$[i]	0.13	0.13	0.13	0.13
Σdicbx/mg L^{-1}[j]	300	300	300	300
Σm_{dicbx}[j]	0.0029	0.0029	0.0029	0.0029
$\Sigma m_{Cl}/\Sigma m_{cbx}$	23	23	23	23
$\Sigma m_{monocbx}/\Sigma m_{dicbx}$	45	45	45	45
Pb/mg L^{-1}[k]	65	0.001	0.02	65
Pb/mg L^{-1} range[l]	Fig. 2	Fig. 2	Fig. 2	Fig. 2
Zn/mg L^{-1}[k]	420	0.002	0.02	420
Zn/mg L^{-1} range[l]	Fig. 3	Fig. 3	Fig. 3	Fig. 3

Modern petroleum field brines[b]

Parameter	Low ΣH_2S, high trace metal content	Low ΣH_2S, low trace metal content	High ΣH_2S, low trace metal content
T/°C	50 to 250	50 to 250	50 to 250
TDS/mg L^{-1}	100 000 to 330 000	20 000 to 330 000	20 000 to 330 000
ΣCl^-/mg L^{-1}	60 000 to 210 000	12 000 to 210 000	12 000 to 210 000
pH	4 to 6.5	4 to 8	4 to 8
ΣH_2S/mg L^{-1}[g]	<0.1	<1.0	1.0 to 1000
Σm_{H_2S}[g]	$<10^{-5.5}$	$<10^{-4.5}$	$10^{-4.5}$ to $10^{-1.4}$
ΣSO_4/mg L^{-1}[h]	0.1 to 1000	0.1 to 1000	0.1 to 1000
Σm_{SO_4}[h]	10^{-6} to 10^{-2}	10^{-6} to 10^{-2}	10^{-6} to 10^{-2}
Σmonocbx/mg L^{-1}[i]	<1.0 to 300	<1.0 to 10 000	<1.0 to 10 000
$\Sigma m_{monocbx}$[i]	$<10^{-4.8}$ to 0.005	$<10^{-4.8}$ to ~ 0.15	$<10^{-4.8}$ to ~ 0.15
Σdicbx/mg L^{-1}[j]	<1.0	<1.0 to 2600	<1.0 to 2600
Σm_{dicbx}[j]	$<10^{-5}$	$<10^{-5}$ to 0.025	$<10^{-5}$ to 0.025
$\Sigma m_{Cl}/\Sigma m_{cbx}$	>340	8 to >1000	8 to >1000
$\Sigma m_{monocbx}/\Sigma m_{dicbx}$	~ 30 to 300	>20	>20
Pb/mg L^{-1}[k]	5 to 70 (cluster)	<0.1 (cluster)	<0.1 (cluster)
Pb/mg L^{-1} range[l]	1 to 111	BDL to 0.9	BDL to 0.9
Zn/mg L^{-1}[k]	15 to 250 (cluster)	<1.0 (cluster)	<0.1 (cluster)
Zn/mg L^{-1} range[l]	1 to 575	BDL to 0.9	BDL to 0.9

[a] Table 1 and Fig. 1 through 5. [b] Rittenhouse *et al.*,[98] Billings *et al.*,[99] Hitchon *et al.*,[100,101] Collins,[102] Carpenter *et al.*,[57] Carpenter and Trout,[103] Kharaka,[104] Kharaka *et al.*,[79,105,106] Land *et al.*,[107] Saunders and Swann,[108] Moldovanyi and Walter,[109] Kyle,[110] Lundegard and Kharaka,[78] Hanor,[59,60,61,62,111,112] Land,[113] Polandri and Reed.[114] [c] pH = 6.0, log $f_{O_2} = -50.0$ [d] pH = 7.5, log $f_{O_2} = -57.0$ [e] pH = 4.7, log $f_{O_2} = -51.8$ [f] pH = 6.0, log $f_{O_2} = -50.0$ [g] Total dissolved inorganic sulfide defined as $\Sigma H_2S = H_2S + HS^-$ (mg L^{-1}) and $\Sigma m_{H_2S} = m_{H_2S} + m_{HS}$ (mol kg^{-1}). [h] Total dissolved sulfate defined as the sum of all dissolved sulfate species in mg L^{-1}(ΣSO_4) and as the molal sum of all dissolved sulfate species (Σm_{SO_4}) in mol kg^{-1}. [i] Monocbx = sum of monocarboxylate anions listed in Table 2: Σmonocbx = total dissolved monocbx in mg L^{-1}; $\Sigma m_{monocbx}$ = total molality of dissolved monocbx in mol kg^{-1}. [j] dicbx = sum of dicarbonxylate anions listed in Table 2: Σdicbx = total dissolved dicbx in mg L^{-1}; Σm_{dicbx} = total molality of dissolved dicbx in mol kg^{-1}. [k] For composite ore-brine; the metal concentration at indicated log f_{O_2}–pH conditions. Cluster = most common values observed for modern petroleum field brines. [l] BDL = below detection limit; less than about 0.01 mg L^{-1}.

summarized in Table 10 for modern petroleum-field brines and for the four-modelled ore fluids considered in this study. The Σm_{H_2S} of the system will of course be controlled by the log f_{O_2}–pH conditions of the brine, assuming sulfate–sulfide equilibrium among the sulfur-bearing species of the system.

Modern petroleum-field brines: composition and types

Excellent summaries of the origin of sedimentary basin brines and their chemical evolution are given by Carpenter,[115] Hanor,[59,60] Kharaka *et al.*,[116] and Kharaka.[104] The compositional data gathered over the past 40 years from sedimentary basins worldwide provide unequivocal evidence that deep formation waters, in particular petroleum-field brines, vary widely in composition (White,[117] Billings *et al.*,[99] Hitchon *et al.*,[100] Collins,[102] Carpenter,[115] Hanor,[59,60,61,62,111,112,118] Kharaka,[104] Kharaka *et al.*,[106,116] Land *et al.*,[107] McManus and Hanor,[119] Wilson and Long,[120] Kyle,[110] Land,[113] Palandri and Reed[114]). This diversity is particularly evident for those variables that significantly influence carboxylate complexation of metals in these fluids. Of particular interest to this study are those modern formation waters classified as Na–Cl and Na–Ca–Cl brines, because of their compositional similarity to inclusion fluids from Mississippi Valley- type and red-bed related base metal deposits (Roedder,[96] Heijlen *et al.*[67]). In Table 10, the model ore fluids considered in this paper are compared to modern Na–Cl and Na–Ca–Cl brines in terms of specific fluid parameters that influence the concentration of Pb and Zn in these waters. In the discussion that follows salinity is defined as total dissolved solids, TDS, in units of milligrams per liter and chlorinity is defined as total chloride in units of milligrams per liter. The salinity of a Na–Cl or Na–Ca–Cl brine

can be estimated from its chlorinity by the relation salinity = 1.7 chlorinity (Hanor[61]). This relation is based on the Cl to NaCl mass ratio of the brine and, therefore, with decreasing Na/Ca values, this estimate becomes less accurate. Nevertheless, it provides a quick conversion between salinity and chlorinity for the brines considered in this study.

Chloride is the dominant anion in formation waters with salinities greater than 20 000 mg L^{-1}, while a transition zone between 20 000 and 10 000 mg L^{-1} defines a TDS boundary below which the dominant anion is either bicarbonate, sulfate, or acetate (Hanor[61,112]). Sodium is the dominant cation in basinal brines with salinities less than 300 000 mg L^{-1}. In general, the relative proportion of Na to K, Ca, or Mg decreases in these waters with increasing salinity and Ca is the dominant cation in basinal brines having salinities in excess of 330 000 mg L^{-1} TDS. Between 300 000 and 330 000 mg L^{-1} TDS, the dominant cation is either Na or Ca. Although salinities generally increase with depth in a sedimentary basin, there are many exceptions to this trend. Thus, the salinity of a formation water is not necessarily related to temperature or pressure.

True *in situ* pHs of deep subsurface brines are not will known (Hanor[61]) and must be estimated from field pH measurements or calculated using a field pH and various assumptions regarding the mineral saturation state of the fluid and loss of volatiles (*e.g.*, H_2S and CO_2) during sampling (Kharaka *et al.*,[105,116] Aggarwal *et al.*,[121] Palandri and Reed[114]). In general, the pH of formation waters decreases with increasing salinity from values of approximately 8 for salinities near 20 000 mg L^{-1} to values between 3 and 4 for halite-saturated brines with salinities near 330 000 mg L^{-1} (Hanor[59,61]). The available field evidence suggests that most Na–Cl and Na–Ca–Cl brines have a pH in the 4-8 range.

The distribution of modern petroleum-field brines in terms of total reduced sulfur content (ΣH_2S) is bimodal in character (Table 10). Low H_2S brines have ΣH_2S values less than 1.0 mg L^{-1}, however, most have ΣH_2S concentrations less than 0.02 mg L^{-1} and often have values below the detection limit of the analytical instrument used (Kharaka *et al.*,[106] Moldovanyi and Walter,[109] Hanor[111]). High H_2S brines have ΣH_2S concentrations greater than 1.0 mg $L^{-1}$with the highest concentrations approaching 1000 mg L^{-1} (Wade *et al.*,[122] Moldovanyi and Walter[109]). The most commonly observed ΣH_2S concentrations from high H_2S formation waters appear to be in the 10 to 600 mg L^{-1} range. Total sulfate concentrations in modern petroleum-field brines (Table 10) rarely exceed 1000 mg L^{-1} and are more typically in the 0.1 to 250 mg L^{-1} range (Kharaka *et al.*,[106] Hanor[111]). Although there appears to be a rough inverse correlation between ΣH_2S and ΣSO_4, there is no statistical correlation between the concentration of SO_4^{2-} and chlorinity or salinity (Hanor[61,111]).

Monocarboxylate anions (mainly acetate, propionate, butyrate, valerate) and dicarboxylate anions (mainly malonate, succinate, glutarate, maleate) are the dominant organic acid species in basinal brines. These species are commonly detected in formation waters associated with petroleum and obtained from reservoirs with temperatures ranging from 20 to 200 °C (Kharaka *et al.*[79]). Concentrations of carboxylic acid anions in modern petroleum-field brines (Tables 2 and 10) are highly variable with respect to their major known controls, including age and temperature of reservoir rocks, type and amount of kerogen in source rocks, and the nature of metastable equilibria that characterized organic-matter interactions in the reservoir (Kharaka,[106] Shock,[1,123] Lundegard and Kharaka,[78] Giordano and Kharaka,[51] Franks *et al.*,[124] Seewald[125]). Although concentrations vary with temperature and reservoir depth for any given petroleum field, maximum values are generally present in Cenozoic-age reservoir rocks in the temperature range 80 to 120 °C (Hanor,[111] Kharaka *et al.*,[79] Lundegard and Kharaka[78]). Based on carboxylate anion concentration *versus* salinity relationships for petroleum-field brines worldwide, Hanor[111] has shown that there is a pronounced decrease in carboxylate anion concentration with increasing salinity. The highest concentrations of carboxylic acid anions are found in waters having salinities less than about 30 000 mg L^{-1}, while these species do not appear to be major constituents of petroleum-field brines having salinities that exceed 100 000 mg L^{-1}.

The total concentration of monocarboxylate anions (Σmonocbx) in modern petroleum-field brines is generally less than 100 mg L^{-1}, however, many brines have concentrations in the 100 to 5000 mg L^{-1} range. The dominant monocarboxylate anion in most petroleum-field brines is acetate, followed in order of decreasing concentration by propionate, butyrate, and valerate (Table 2). The highest concentration of acetate reported is 10 000 mg L^{-1} but values higher than 5000 mg L^{-1} are very rare (Lundegard and Kharaka,[78] Kharaka *et al.*[79]). Typically acetate comprises 80 to 90% of the total monocarboxylate species (Giordano and Kharaka[51]). The dominant dicarboxylate species in modern petroleum-field brines are malonate, succinate, and glutarate. Each of these species is not likely to have concentrations greater than about 100 mg L^{-1} (Table 2), but controversially high values for oxalate (494 mg L^{-1}) and malonate (2540 mg L^{-1}) have been reported (MacGowan and Surdam[126]). Reported total dicarboxylate anion concentrations (Σdicbx) range from 0 to 2640 mg L^{-1} but values higher than 300 mg L^{-1} are very rare.

Typically, brines high in dicarboxylate anions are also high in monocarboxylate anions; however, brines high in monocarboxylate species are not always enriched in dicarboxylate anions. The total dicarboxylate anion concentration is typically less than 5% of the total carboxylate concentration for modern petroleum-field brines. Thus, the ratio of total monocarboxylate anions to total dicarboxylate anions ($\Sigma m_{\text{monocbx}}/\Sigma m_{\text{dicbx}}$) for modern basinal brines is nearly always greater than 20.

Modern petroleum-field brines: Pb and Zn content

The speciation results from this study show that deep formation waters characterized by temperatures near 100 °C, high oxidation states (*i.e.*, low Σm_{H_2S}), high chlorinities ($\sim$100 000 mg L^{-1}), and high but reasonable concentrations of carboxylate anions can mobilize up to 3% of the total Pb and up to 1.3% of the total Zn as carboxylate complexes. Furthermore, these percentages, under the most favorable conditions, correspond to approximately 1 to 100 ppm of these metals in solution; concentrations that are adequate to form economic deposits of these metals. However, the field evidence suggests that all of these optimum conditions for carboxylate complexation are rarely met at the same time and that total concentrations of Pb and Zn are typically below 0.1 mg L^{-1} in most oil-field brines (Kharaka *et al.*[105,106]). Nevertheless, as indicated in Table 10, formation waters high in trace metal content are common in a dozen or so localities worldwide (Carpenter *et al.*,[57] Kharaka,[104] Kharaka *et al.*,[105,106] Saunders and Swann,[108] Moldovanyi and Walter,[109] Kyle,[110] Land,[113] Hanor,[59,61,62] Hitchon *et al.*[101]). These brines typically have concentrations of Pb and Zn in the 1 to 250 mg L^{-1} range, with maximum reported concentrations of 111 mg L^{-1} and 575 mg L^{-1} for Pb and Zn, respectively (Table 10).

To ascertain the factors influencing base metal concentrations in deep formation waters, the compositional data from a large number of modern petroleum-field brines, worldwide, have been evaluated by many investigators using a variety of correlation and chemical modelling methods (Sverjensky,[31,41] Kharaka *et al.*,[106,116,127] Lundegard and Kharaka,[128] Giordano and Kharaka,[51] Hanor,[60,62,111,112] Hitchon *et al.*,[101] Palandri and Reed[114]). Based on these studies as well as others, it is now well established that three principal factors control Pb and Zn concentrations in modern basinal brines: (1) the availability of Pb and Zn in the basinal system, (2) the total reduced sulfide

content (ΣH_2S) of the brine, and (3) the chlorinity of the brine (ΣCl^-).

The field evidence for modern petroleum-field brines, as summarized in Table 10, suggests an inverse relationship between total sulfide content and the concentration of Pb and Zn. All high ΣH_2S brines have low concentrations of these metals, while all brines with elevated Pb and Zn values have low concentrations of total sulfide. General details of this inverse relation are presented by Kharaka *et al.*,[106] Moldovanyi and Walter,[109] and Hanor.[61] Hanor[61] also reports a pronounced covariation in Zn and Pb corresponding to a mass ratio of approximately 5 : 1 for brines with dissolved Zn concentrations greater than a few mg L^{-1}, while there is considerable scatter in Zn to Pb ratios for brines having Zn and Pb concentrations below 1 mg L^{-1}. These relationships (Zn + Pb *vs.* ΣH_2S and Zn *vs.* Pb) support the conclusion that one control of Pb concentration and Zn concentration in high trace-metal brines is mineral buffering, possibly equilibrium with galena and sphalerite, respectively (Kharaka *et al.*,[106] Hanor[61,62]).

However, because most low ΣH_2S petroleum-field brines also have low concentrations of trace metals (*e.g.*, Pb and Zn < 1.0 mg L^{-1} each, see Table 10) and highly variable Zn to Pb ratios, the availability of Pb and Zn in the brines must also be a major control on the concentration these metals. Because galena and sphalerite are normally not present as components of basinal sediments, it seems more likely that Pb and Zn in most petroleum-field waters (as well as related ore fluids) were ultimately leached from other sources including metal oxides and hydroxides associated with red-bed sediments, organic matter, K-feldspar in sandstone, carbonate phases, or shales (Sverjensky,[31,41] Kharaka *et al.*,[106] Hanor[61]). If such is the case, then it is not surprising that most low ΣH_2S formation waters with low concentration of Pb and Zn are also characterized by variable Zn to Pb ratios.

Both field and modelling evidence demonstrate that chlorinity has a strong influence on the trace metal content of petroleum-field brines (Lundegard and Kharaka,[128] Hanor,[60,61,111] Kharaka *et al.*[79]). The relationship of chlorinity *versus* Zn concentration for Gulf Coast saline waters (Hanor[61]) shows unequivocally that petroleum-field brines which have Pb and Zn concentrations in excess of 1.0 mg L^{-1} nearly always have chlorinities in excess of approximately 100 000 mg L^{-1} (salinity = 170 000 mg L^{-1}). There is a ΣCl^- transition zone between 60 000 mg L^{-1} (salinity = 100 000 mg L^{-1}) and 100 000 mg L^{-1} in which a few brines have Pb or Zn in excess of 1 mg L^{-1}. As mentioned by Hanor,[61,111] these results strongly suggest a threshold chlorinity of roughly 100 000 mg L^{-1} below which formation waters are typically poor solvents of Pb and Zn and above which Pb and Zn, in concentrations capable of forming economic deposits of these metals, can be mobilized by formation waters. These field relationships are consistent with modelling results, including those of this study, which show that chloride complexing is the principal solubility mechanism for Pb and Zn in low ΣH_2S petroleum-field brines and is probably the principal solubility mechanism for these metals in related ore fluids (*cf.*, Sverjensky,[31, 41] Kharaka *et al.*,[79,106] Lundegard and Kharaka,[128] Giordano and Kharaka,[51] Hanor[61,62]).

Model ore fluids

A comparison of the composite ore fluid compositions from this study (Table 10 and related isopleths in Fig. 2 and 3) and the modern brine data in Table 10 shows that the ore brines, corresponding to log f_{O_2}–pH conditions based on the Anderson[37] and Giordano[76] model fluids, are similar in many respects to modern, high trace-metal petroleum-field brines. Both sets of fluids have the following characteristics in common: (a) chlorinities (ΣCl^-) near 100 000 mg L^{-1} or higher, (b) pH in the 4–6.5 range, (c) less than 0.1 mg L^{-1} total sulfide (ΣH_2S), (d) total sulfate (ΣSO_4) in the 0.1 to 1000 mg L^{-1} range, and (e) Pb concentrations in the 1 to 100 mg L^{-1}range and Zn concentrations in the 1 to 1000 mg L^{-1} range. Note that the Pb and Zn isopleths transecting the more reduced log f_{O_2}–pH regions of the Anderson[37] and Giordano[76] ore fluids in Fig. 2 and 3, as well as the Pb content (65 mg L^{-1}) and Zn content (420 mg L^{-1}) for the corresponding composite fluids in Table 10, are close to the highest concentrations reported for these metals in petroleum-field brines (Pb, 111 mg L^{-1}; Zn, 575 mg L^{-1}). Also note that the 1 mg L^{-1} minimum for Pb and Zn in high trace-metal brines is consistent with the 1ppm Pb and 1 ppm Zn isopleths in Fig. 2 and 3, that are not far from the lower boundary of the Anderson[37] and Giordano[76] ore-regions.

The modelled fluids in this study are in equilibrium with galena and sphalerite. Hence, the above similarities in Pb and Zn content between the composite ore fluids and modern high trace-metal brines is consistent with the above assertion that an important control of Pb and Zn content in high trace-metal brines is mineral buffering, most likely equilibrium with galena and sphalerite. However, as mentioned by other investigators (Sverjensky,[31,41] Kharaka *et al.*,[106] Hanor[61]), it is likely that the original sources for much of the dissolved Pb and Zn in metal-rich brines are phases other than galena and sphalerite; including organic matter, oxides, hydroxides, silicates, and carbonates. The principal differences between modern high trace-metal brines and the composite ore fluids of Anderson[37] and Giordano[76] relate to their carboxylate anion content (Table 10). The reported concentrations of monocarboxylate anions (Σmonocbx) and dicarboxylate anions (Σdicbx) in high trace-metal petroleum-field brines (<1 to 300 mg L^{-1} and <1 mg L^{-1}, respectively) are significantly lower than the concentrations assumed in the modelled brines of this study (Σmonocbx = 7 700 mg L^{-1} and Σdicbx = 300 mg L^{-1}). Also, the ratio of monocarboxylate acid anions to dicarboxylate ligand species (Σmonocbx/Σdicbx) appears to be higher in modern high trace-metal brines compared to the composite ore fluid. These systematics in organic acid content suggest that carboxylate complexation of Pb and Zn in modern brines should be less than predicted by the composite brine modal in this study. There are also major differences in the corresponding total chloride to carboxylate ratio ($\Sigma m_{Cl}/\Sigma m_{cbx}$). Modern high trace-metal brines have much higher $\Sigma m_{Cl}/\Sigma m_{cbx}$ values and, therefore, the contribution carboxylate complexes to the total Pb and Zn content in these modern brines is likely to be significantly less than the 1 to 3 percent for the composite ore fluids of Anderson[37] and Giordano[76] (). This is consistant with the prediction of Giordano and Drummond[87] that zinc chloride complexes dominate over acetate complexes of Zn if $\Sigma m_{Cl}/\Sigma m_{acetate}$ is greater than 10 at temperatures near 100 °C.

In contrast to these ore solutions, the composite ore-brine based on the Giordano and Barnes[39] MVT ore fluid (Table 10, Fig. 2 and 3) is comparable to the high salinity (>170 000 mg L^{-1} TDS) subset of modern brines characterized by low trace-metal content and high total reduced sulfur (ΣH_2S) (Table 10, bottom half, right column). The Giordano and Barnes[39] composite fluid is saturated with respect to galena and sphalerite and Pb and Zn speciation is dominated by sulfide complexes (Tables 5, 6, 8, 9). Thus, it is likely that concentrations of Pb and Zn in modern low trace-metal brines, with high sulfide content and slightly acidic to alkaline in pH, are also controlled by galena and sphalerite solubility and sulfide complexation of Pb^{2+} and Zn^{2+}. Overall concentrations of Pb and Zn are low because of the high sulfide content and, hence, the activities of Pb^{2+} and Zn^{2+} are suppressed because of mass action effects. It is likely that carboxylate complexation of Pb and Zn is insignificant in these fluids because of the presumably low concentration of carboxylate ligands and because Pb^{2+} and Zn^{2+} activities are low, thus suppressing the formation of

carboxylate complexes, which are significantly weaker that sulfide complexes. Although high concentrations of carboxylate anions have been observed in certain high ΣH_2S petroleum-field brines, these high concentrations are always from brines with salinities much lower than 170 000 mg L^{-1} TDS.

A comparison of the Sverjensky composite ore-brine[41] with modern petroleum-field brines in terms of ΣH_2S and Zn content, revels that this ore fluid holds a border position between modern high trace-metal brines and those with low trace-metal content and high ΣH_2S (Table 10). The composite Sverjensky fluid, as represented by the model results in Table 10 and Fig. 2 and 3, barely qualifies as a modern low trace-metal/high ΣH_2S brine and it is not far removed from modern high trace-metal brines that have total Zn content and ΣH_2S near the lower limit (1 mg L^{-1}) and upper limit (0.1 mg L^{-1}), respectively, for this brine category. As mentioned above, both of these modern brine-types are probably saturated, or close to saturation, with respect to galena and sphalerite. Also, these two modern brine-types generally coincide when ΣH_2S, Zn, and/or Pb all have values within or near the 1 to 10 mg L^{-1} range. Thus, modern brines having these characteristics are referred to below as border-type brines.

Based on brine-composition data from numerous references cited in this paper, border-type brines do exist but are rare. Hanor[61] discusses the variation of total Zn with ΣH_2S in Gulf Coast formation waters and suggests that brines which contain both dissolved Zn and dissolved total reduced sulfur in the 1 to 10 mg L^{-1} range are probable. He also implies that these brines are likely to be saturated with respect to galena and sphalerite. Hanor[61] also conducted computer simulations of sphalerite solubility, at 100 °C, in hypothetical basinal brines and reports that at chlorinites in excess of 150 000 mg L^{-1} (TDS = 250 000 mg L^{-1}) it may be possible for concentrations of Pb and Zn in excess of 1 mg L^{-1} to coexist in solution with comparable concentrations of dissolved inorganic sulfide. It is interesting to note that the original MVT ore fluid of Sverjensky[41] is initially saturated with respect to galena, but undersaturated with respect to sphalerite and contains 1.3 mg L^{-1} Zn, 2 mg L^{-1} Pb, and approximately 1 mg L^{-1} dissolved sulfide (ΣH_2S). Thus, Sverjensky's initial MVT ore fluid also corresponds to a border-type brine, as defined above.

The principal compositional difference between the original Sverjensky MVT fluid[41] and the composite Sverjensky brine modelled in this study is in the total sulfur content. The original ore fluid has a total sulfur content of approximately $10^{-4.6}$ molal (1 mg L^{-1}as H_2S), while total sulfur content in the composite fluid of this study is 10^{-2} molal (340 mg L^{-1}as H_2S or 960 mg L^{-1} as SO_4^{2-}). Thus, for the most oxidized and acidic conditions of the composite Sverjensky model, pH near 4.6 and log f_{O_2}near –51.8 (Table 10, Fig. 2 and 3), both ore fluid models, yield similar total Zn and ΣH_2S values, close to those of a border-type brine. However, as log f_{O_2}–pH conditions deviate from this point in terms of log f_{O_2}, but still remain in the delimited ore-fluid region, the composite fluid yields values for ΣH_2S and concentrations of Zn and Pb that are more in line with modern brines high in ΣH_2S and low in trace-metals, while the original model fluid of Sverjensky,[41] remains a border-type brine because the total reduced sulfur content can not increase beyond $10^{-4.6}$ molal, or 1 mg L^{-1} ΣH_2S.

Border-type brines and ore fluids with similar key characteristics, are probably at or near saturation with respect to galena and sphalerite and mobilization of Pb and Zn in these fluids is dominated by either chloride or sulfide complexation, depending on the log f_{O_2}–pH conditions, the chlorinity, and the total dissolved sulfide content. For the more oxidized conditions within the Sverjensky ore-fluid region[41] (Fig. 2 to 5, Tables 5 and 8), chloride complexation dominates Pb and Zn solubility, with only a few percent of the total Pb and Zn being transported by carboxylate complexes. Under more reduced conditions, sulfide complexation of Pb and Zn dominates transport of these metals and, once again, carboxylate complexes are insignificant.

Geochemical modelling of petroleum-field brines

The model results and field evidence presented above are consistent with chemical simulation studies of carboxylate complexation in modern petroleum-field brines. (*cf.*, Kharaka *et al.*,[79,105,106,116,127] Lundegard and Kharaka,[128] Giordano and Kharaka[51]). The results from these studies indicated (1) that concentrations of Pb and Zn in carboxylate complexes form only a small percentage of the total Pb and Zn in metal-rich petroleum-field brines, (2) chloride complexation dominates Pb and Zn speciation in these brines, and (3) significant amounts of Ca, Mg, Fe, and Al can be complexed by carboxylate ligands in petroleum-field brines. The influence of pH and oxygen fugacity on the solubilization of Ca, Mg, Al, and Fe by carboxylate complexes in fluids similar to those modelled in this study is currently being investigated by the author and results of this study will be the topic of a forthcoming paper.

Conclusions

The chemical simulation results from this study and the comparisons made between proposed ore fluids and modern brines lead to several important conclusions regarding the role of carboxylate complexation of Pb and Zn in Mississippi Valley-type (MVT) ore fluids, ore fluids responsible for red-bed related base metal(RBRBM) deposits, and modern petroleum-field brines.

(1) A comparison of dissolved Pb, Zn and sulfur content of modern petroleum-field brines with Pb and Zn solubility systematics in log f_{O_2}–pH space for the composite ore-brine in this study reveals good correlations between modern brine-types and proposed ore fluid models for Mississippi Valley-type deposits and red-bed related base metal deposits.

(2) Based on analyses of formation waters worldwide and the modeling results of this study, modern petroleum-field brines and the model ore fluids can be divided into four main categories:

(a) High trace-metal, low total sulfide brines which are similar to the 1975 model MVT fluid of Anderson[37] and the 1994 RBRBM ore fluid of Giordano.[76] Total sulfide is less than 0.1 mg L^{-1}, while total Pb and Zn have values between 1 and 100 mg L^{-1} and 1 and 1000 mg L^{-1}, respectively.

(b) Low trace-metal, high total sulfide brines which are similar to the 1981 MVT ore fluid of Giordano and Barnes.[39] Total sulfide is between 1 and 1000 mg L^{-1}, while total Pb and Zn are normally less than 0.1 mg L^{-1}.

(c) Low trace-metal, low total sulfide brines which may correlate to spent ore fluids or to basinal fluids not sufficiently enriched in Pb or Zn to be ore fluids of these metals.

(d) Border-type brines that in terms of reduced sulfur and trace metal content are on the border between high trace-metal brines and brines low in trace metals but high in sulfide. Brine-types (a) and (b) above coincide when total sulfide, total Pb, and/or total Zn all have values near or within the 1 to 10 mg L^{-1} range. Brines of this type are rare and generally correspond to the 1984 model ore fluid of Sverjensky.[41]

(3) In modern basinal brines and related ore fluids with chlorinites near 100 000 mg L^{-1}, chloride complexes dominate the speciation of Pb and Zn under log f_{O_2}–pH conditions most favorable for the complexation of these metals by carboxylate ligands.

(4) The model results at 100 °C indicate that, for these basinal brines under the most favorable conditions, up to 3% of the total Pb and up to 1.3% of the total Zn can be mobilized by

carboxylate complexes, principally those involving the acetate ligand.

(5) The percent of dissolved Zn and Pb complexed by carboxylate ligands in a basinal brine will depend primarily on four key variables, assuming a system remains invariant with respect to temperature, total sulfur content of the brine, and mineralogy of the aquifer. The four variables are (a) the ratio of total chloride molality to total carboxylate ligand molality, (b) the mix of specific carboxylate ligands, for example the molar ratio of monocarboxylate ligands to dicarboxylate ligands, (c) the concentration of total sulfide, which is controlled by the log f_{O_2}–pH conditions of the brine, assuming sulfate–sulfide equilibrium among the sulfur-bearing species of the system, and (d) pH.

(6) Optimum brine conditions, at 100 °C, for carboxylate complexation include (a) high oxidation state, reflecting a high total sulfate to total sulfide ratio and total sulfide concentrations less than 10^{-6} molal (< 0.03 mg L^{-1} as dissolved H_2S), (b) high but reasonable concentrations of carboxylate anions; near 7000 mg L^{-1} for total monocarboxylate species and 300 mg L^{-1} for total dicarboxylate ligands, and (c) pH in the 4–8 range.

(7) At 100 °C, under optimum brine conditions for carboxylate complexation, approximately 1 to 100 mg L^{-1} and 0.1 to 10 mg L^{-1} of Zn and Pb, respectively, can be mobilized as carboxylate complexes, principally those involving acetate.

(8) However, the field evidence based on analyses of petroleum-field brines worldwide, suggests that all of these optimum conditions are rarely, if ever, met at the same time, particularly with regard to the requisite carboxylate ligand content. Thus, it appears that carboxylate complexation plays a minor, if not insignificant, role as a transport mechanism for Pb and Zn in high salinity Na–Cl and Na–Ca–Cl basinal brines and related ore fluids.

(9) More refined simulations of base-metal solubility and speciation in basinal brines can be conducted by making the following modifications of the model used in this study: (a) the use of reliable 100 °C thermodynamic data for Pb^{2+} and Zn^{2+} malonate complexes, (b) the inclusion of Cu^{+} complexation in the model, (c) better estimates of log f_{O_2} and pH conditions for the modelled ore fluids and modern petroleum-field brines, and (d) the use of mineral solubility constraints to control the activities of Na^{+}, Ca^{2+}, and Mg^{2+} in the model.

References

1 E. L. Shock, Organic acid metastability in sedimentary basins, *Geology*, 1988, **16**, 886–890.
2 E. L. Shock, Corrections to "Organic acid metastability in sedimentary basins", *Geology*, 1989, **17**, 572–573.
3 E. L. Shock, Thermodynamic response of organic compounds in geochemical processes of sedimentary basins, *Rev. Econ. Geol.*, 2000, **9**, 119–131.
4 H. C. Helgeson, A. M. Knox, C. E. Owens and E. L. Shock, Petroleum, oil field waters, and authigenic mineral assemblages: Are they in metastable equilibrium in hydrocarbon reservoirs? *Geochim. Cosmochim. Acta*, 1993, **57**, 3295–3339.
5 H. L. Barnes and G. Kullerud, Equilibria in sulfur-containing aqueous solutions, in the system Fe–S–O, and their correlation during ore deposition, *Econ. Geol.*, 1961, **56**, 648–688.
6 H. L. Barnes and G. K. Czamanske, Solubilities and transport of ore minerals, in *Geochemistry of Hydrothermal Ore Deposits*, ed. H. L. Barnes, Holt, Rinehart and Winston, New York, 1967, pp. 334–381.
7 E. M. Ripley and H. Ohmoto, A FORTRAN program for plotting mineral stabilities in the Fe–Cu–S–O system in terms of log ($\Sigma SO_4/\Sigma H_2S$) or log f_{O_2} *vs.* pH or *T*, *Comput. Geosci.*, 1979, **5**, 289–300.
8 R. W. Henley, A. H. Truesdell, P. B. Barton and J. A. Whitney, Fluid–Mineral Equilibria in Hydrothermal Systems, *Rev. Econ. Geol.*, 1984, **1**, 267.
9 D. C. McPhail, Thermodynamic properties of aqueous tellurium species between 25 and 350 °C, *Geochim. Cosmochim. Acta*, 1995, **59**, 851–566.
10 S. A. Wood, Calculation of activity and log f_{O_2}–pH diagrams, *Rev. Econ. Geol.*, 1998, **10**, 81–96.
11 H. Ohmoto, Systematics of sulfur and carbon isotopes in hydrothermal ore deposits, *Econ. Geol.*, 1972, **67**, 551–578.
12 H. Ohmoto and R. O. Rye, Isotopes of sulfur and carbon, in *Geochemistry of Hydrothermal Ore Deposits*, ed. H. L. Barnes, Wiley, New York, 2nd edn., 1979, pp. 509–567.
13 X. Zhang, SULF34: A QUICKBASIC program for calculating sulfur isotope distribution in log f_{O_2}–pH diagram, *Comput. Geosci.*, 1993, **19**, 817–823.
14 A. P. Gize, Organic alteration in hydrothermal sulfide ore deposits, *Econ. Geol.*, 1999, **94**, 967–980.
15 E. M. Ripley and H. Ohmoto, Mineralogic, sulfur isotope, and fluid inclusion studies of the stratabound copper deposits at the Raul mine, Peru, *Econ. Geol.*, 1977, **72**, 1017–1041.
16 M. Ahmad, M. Solomon and J. L. Walshe, Mineralogical and geochemical studies of the Emperor gold telluride deposit, Fiji, *Econ. Geol.*, 1987, **82**, 345–370.
17 H. Ohmoto and M. B Goldhaber, Sulfur and carbon isotopes, in *Geochemistry of Hydrothermal Ore Deposits*, ed. H. L. Barnes, Wiley, New York, 3rd edn., 1997, pp. 517–611.
18 H. Ohmoto, M. Mizukami, S. E. Drummond, C. S. Eldridge, V. Pisutha-Arnond and T. C. Lenagh, Chemical processes of Kuroko Formation, in *The Kuroko and Related Volcanogenic Massive Sulfide Deposits*, ed. H. Ohmoto and B. J. Skinner, Society of Economic Geologists, Monograph 5, 1983, pp. 570–604.
19 H. P. Eugster, Minerals in hot water, *Am. Mineral.*, 1986, **71**, 655–673.
20 W. F. Giggenbach, The origin and evolution of fluids in magmatic–hydrothermal systems, in *Geochemistry of Hydrothermal Ore Deposits*, ed. H. L. Barnes, Wiley, New York, 3rd edn., 1997, pp. 737–796.
21 D. R. Cooke, S. W. Bull, R. R. Large and P. J. McGoldrick, The importance of oxidized brines for the formation of Australian Proterozoic stratiform sediment-hosted Pb–Zn (Sedex) deposits, *Econ. Geol.*, 2000, **95**, 1–17.
22 S. A. Wood and I. M. Samson, The hydrothermal geochemistry of tungsten in granitoid environments: I. Relative solubilities of ferberite and scheelite as a function of *T*, *P*, pH, and m_{NaCl}, *Econ. Geol.*, 2000, **95**, 143–179.
23 A. W. Rose, The effect of cuprous chloride complexes in the origin of red-bed copper and related deposits, *Econ. Geol.*, 1976, **71**, 1036–1048.
24 A. W. Rose, Mobility of copper and other heavy metals in sedimentary environments, in *Sediment-Hosted Stratiform Copper Deposits, Geological Association of Canada Special Paper 36*, ed. R. W. Boyle, A. C. Brown, C. W. Jefferson, E. C. Jowett and R. V. Kirkham, Geological Association of Canada, 1989, pp. 97–110.
25 R. P. Wintsch, Supercritical pE–pH diagrams with applications to the stability of biotite, *Contrib. Mineral. Petrol*, 1980, **73**, 421–428.
26 B. G. Pound, G. A. Wright and R. M. Sharp, Electrochemical phase diagrams for Fe/S/H_2O system under geothermal conditions, *Aust. J. Chem.*, 1985, **38**, 643–657.
27 M. Pourbaix and A. Pourbaix, Potential–pH equilibrium diagrams for the systems S–H_2O from 25 to 150 °C: Influence of access of oxygen in sulfide solutions, *Geochim. Cosmochim. Acta*, 1992, **56**, 3157–3178.
28 R. M. Kettler, G. S. Waldo, J. E. Penner-Hahn, P. A. Meyers and S. E. Kesler, Sulfidation of organic matter associated with gold mineralization, Pueblo Viejo, Dominican Republic, *Appl. Geochem.*, 1990, **5**, 237–248.
29 P. B. Barton, P. M. Bethke and E. Roedder, Environment of ore deposition in the Creede Mining District, San Juan Mountains, Colorado: Part III. Progress toward interpretation of the chemistry of the ore-forming fluid of the OH vein, *Econ. Geol.*, 1977, **72**, 1–24.
30 T. Casadevall and H. Ohmoto, Sunnyside mine, Eureke mining district, San Juan County, Colorado: Geochemistry of gold and base metal ore deposition in a volcanic environment, *Econ. Geol.*, 1977, **72**, 1285–1320.
31 D. A. Sverjensky, The role of migrating oil field brines in the formation of sediment –hosted Cu-rich deposits, *Econ. Geol.*, 1987, **82**, 1130–1141.
32 D. A. Sverjensky, Chemical evolution of basinal brines that formed sediment-hosted Cu–Pb–Zn deposits, in *Sediment-Hosted Stratiform Copper Deposits, Geological Association of Canada*

Special Paper 36, ed. R. W. Boyle, A. C. Brown, C. W. Jefferson, E. C. Jowett and R. V. Kirkham, Geological Association of Canada, 1989, pp. 127–134.
33 T. M. Seward and H. L. Barnes, Metal transport by hydrothermal ore fluids, in *Geochemistry of Hydrothermal Ore Deposits*, ed. H. L. Barnes, Wiley, New York, 3rd edn., 1997, pp. 435–486.
34 J. T. Wells and M. S. Ghiorso, Rock alteration, mercury transport, and metal deposition at Sulphur Bank, California, *Econ. Geol.*, 1988, **83**, 606–618.
35 H. L. Barnes and T. M. Seward, Geothermal systems and mercury deposits, in *Geochemistry of Hydrothermal Ore Deposits*, ed. H. L. Barnes, Wiley, New York, 3rd edn., 1997, pp. 699–736.
36 J. B. Fein and A. E. Williams-Jones, The role of mercury–organic interactions in the hydrothermal transport of mercury, *Econ. Geol.*, 1997, **92**, 20–28.
37 G. M. Anderson, Precipitation of Mississippi Valley-type ore fluids, *Econ. Geol.*, 1975, **70**, 937–942.
38 G. M. Anderson, Some geochemical aspects of sulfide precipitation in carbonate rock, in *International Conference on Mississippi Valley Type Lead–Zinc Deposits, Proceedings Volume*, ed. G. Kisvarsanyi, S. K. Grant, W. P. Pratt and J. W. Koenig, University of Missouri, Rolla, 1983, pp. 61–76.
39 T. H. Giordano and H. L. Barnes, Lead transport in Mississippi Valley-type ore solutions, *Econ. Geol.*, 1981, **76**, 2200–2211.
40 H. L. Barnes, Ore-depositing reactions in Mississippi Valley-type deposits, in *International Conference on Mississippi Valley Type Lead–Zinc Deposits, Proceedings Volume*, ed. G. Kisvarsanyi, S. K. Grant, W. P. Pratt and J. W. Koenig, University of Missouri, Rolla, 1983, pp. 77–85.
41 D. A. Sverjensky, Oil field brines as ore-forming solutions, *Econ. Geol.*, 1984, **79**, 23–37.
42 D. A. Crerar and H. L. Barnes, Ore solution chemistry V. Solubilities of chalcopyrite and chalcocite assemblages in hydrothermal solution at 200 to 350 °C, *Econ. Geol.*, 1976, **71**, 772–794.
43 C. H. Gammons and A. E. Williams-Jones, The solubility of Au–Ag alloys + AgCl in HCl/NaCl solutions to 300 °C: New data on the stability of Au(I) chloride complexes in hydrothermal fluids, *Geochim. Cosmochim. Acta*, 1995, **59**, 3453–3468.
44 B. W. Mountain and S. A. Wood, Chemical controls on the solubility, transport, and deposition of platinum and palladium in hydrothermal solutions: A thermodynamic approach, *Econ. Geol.*, 1988, **83**, 492–510.
45 S. A. Wood, B. W. Mountain and B. A. Fenlon, Thermodynamic constraints on the solubility of platinum and palladium in hydrothermal solutions: Reassessment of hydroxide, bisulfide, and ammoniacomplexing, *Econ. Geol.*, 1989, **84**, 2020–2028.
46 C. H. Gammons, M. S. Bloom and Y. Yu, Experimental investigation of the hydrothermal geochemistry of platinum and palladium: I. Solubility of platinum and palladium sulfide minerals in $NaCl/H_2SO_4$ solutions at 300 °C, *Geochim. Cosmochim. Acta*, 1992, **56**, 3881–3894.
47 T. H. Giordano, A preliminary evaluation of organic ligands and metal–organic complexing in Mississippi Valley-type ore solutions, *Econ. Geol.*, 1985, **80**, 96–106.
48 S. E. Drummond and D. A. Palmer, Thermal decarboxylation of acetate. Part II. Boundary conditions for the role of acetate in the primary migration of natural gas and the transportation of metals in hydrothermal systems, *Geochim. Cosmochim. Acta*, 1986, **50**, 825–833.
49 D. A. C. Manning, Assessment of the role of organic matter in ore transport processes in low-temperature base-metal systems, *Trans. - Inst. Min. Metall., Sect. B*, 1986, **95**, 195–200.
50 R. J. C. Hennet, D. A. Crerar and J. Schwartz, Organic complexes in hydrothermal systems, *Econ. Geol.*, 1988, **83**, 742–764.
51 T. H. Giordano and Y. K. Kharaka, Organic ligand distribution and speciation in sedimentary basin brines, diagenetic fluids and related ore solutions, in *Geofluids: Origin, Migration and Evolution of Fluids in Sedimentary Basins, Geol. Soc. Spec. Pub. 78*, ed. J. Parnell, Geological Society, London, 1994, pp. 175–202.
52 A. A. Sicree and H. L. Barnes, Upper Mississippi Valley district ore fluid model: The roles of organic complexes, *Ore Geol. Rev.*, 1996, **11**, 105–131.
53 T. H. Giordano, Organic matter as a transport agent in ore-forming systems, *Rev. Econ. Geol.*, 2000, **9**, 133–155.
54 R. J. C. Hennet, D. A. Crerar and J. Schwartz, The effect of carbon dioxide partial pressure on metal transport in low-temperature hydrothermal systems, *Chem. Geol.*, 1988, **69**, 321–330.
55 J. S. Leventhal and T. H. Giordano, The nature and roles of organic matter associated with ores and ore-forming systems: An introduction, *Rev. Econ. Geol.*, 2000, **9**, 1–26.
56 F. W. Beales and S. A. Jackson, Precipitation of lead–zinc ores in carbonate reservoirs as illustrated by Pine Point ore field, Canada, *Trans. - Inst. Min. Metall., Sect. B*, 1966, **75**, 278–285.
57 A. B. Carpenter, M. L. Trout and E. E. Pickett, Preliminary report on the origin and chemical evolution of lead- and zinc-rich oil field brines in central Mississippi, *Econ. Geol.*, 1974, **69**, 1191–1206.
58 B. Hitchon, Geochemical links between oil fields and ore deposits in sedimentary rocks, in *Proceedings of the Forum on Oil and Ore in Sediments*, 1975, ed. P. Garrard, Imperial College of London, 1977, pp. 1–35.
59 J. S. Hanor, The sedimentary genesis of hydrothermal fluids, in *Geochemistry of Hydrothermal Ore Deposits*, ed. H. L. Barnes, Wiley-Interscience, New York, 2nd edn., 1979, pp. 137–172.
60 J. S. Hanor, Origin of saline fluids in sedimentary basins, in *Geofluids: Origin, Migration and Evolution of Fluids in Sedimentary Basins, Geol. Soc. Spec. Publ. 78*, ed. J. Parnell, Geological Society, London, 1994, pp. 151–174.
61 J. S. Hanor, Controls on the solubilization of lead and zinc in basinal brines, *Soc. Econ. Geol. Spec. Publ. 4*, 1996, 483–500.
62 J. S. Hanor, Geochemistry and origin of metal-rich brines in sedimentary basins, in *Basins, Fluids and Zn–Pb Ores, Spec. Publ. 2*, ed. J. Pongratz and P. McGoldrick, University of Tasmania, Centre for Ore Deposit Research (CODES), 1998, pp. 65–79.
63 G. M. Anderson and R. W. MacQueen, Ore deposit models - 6. Mississippi Valley-type lead–zinc deposits, *Geosci. Can.*, 1982, **9**, 108–117.
64 J. W. Lyndon, Chemical parameters controlling the origin and deposition of sediment-hosted stratiform lead–zinc deposits, in *Short Course in Sediment-Hosted Stratiform Lead–Zinc Deposits, Short Course Handbook 9*, ed. D. F. Sangster, Mineralogical Association of Canada, 1983, pp. 175–250.
65 D. F. Sangster, Mississippi Valley-type and Sedex lead–zinc deposits: a comparative examination, *Trans. - Inst. Min. Metall., Sect. B*, 1990, **99**, 21–42.
66 E. R. Force, J. J. Eidel and J. B. Maynard, Sedimentary and Diagenetic Mineral Deposits: A Basin Analysis Approach to Exploration, *Rev. Econ. Geol.*, 1991, **5**, 216.
67 W. Heijlen, P. Muchez and D. A. Banks, Origin and evolution of high-salinity, Zn–Pb mineralizing fluids in the Variscides of Belgium, *Mineralium Deposita*, 2001, **36**, 165–176.
68 A. Bjorlykke and D. F. Sangster, An overview of sandstone lead deposits and their relation to red-bed copper and carbonate-hosed lead–zinc deposits, in *Economic Geology, 75th Anniversary Volume*, ed. B. J. Skinner, Society of Economic Geologists, Boulder, CO, 1981, pp. 179–213.
69 L. B. Gustafson and N. Williams, Sediment-hosted stratiform deposits of copper, lead, and zinc, in *Economic Geology, 75th Anniversary Volume*, ed. B. J. Skinner, Society of Economic Geologists, Boulder, CO, 1981, pp. 139–278.
70 G. Kisvarsanyi, S. K. Grant, W. P. Pratt and J. W. Koenig, *International Conference on Mississippi Valley Type Lead–Zinc Deposits, Proceedings Volume*, University of Missouri-Rolla, 1983, p. 603.
71 D. A. Sverjensky, Genesis of Mississippi Valley-type lead–zinc deposits, *Annu. Rev. Earth Planet. Sci.*, 1986, **14**, 177–199.
72 D. W. Haynes and M. S. Bloom, Stratiform copper deposits hosted by low-energy sediments: III. Aspects of metal transport, *Econ. Geol.*, 1987, **82**, 635–648.
73 R. W. Boyle, A. C. Brown, C. W. Jefferson, E. C. Jowett and R. V. Kirkham, Sediment-Hosted Stratiform Copper Deposits, *Geol. Assoc. Can. Spec. Pap. 36*, 1989, 710.
74 D. L. Leach and M. B. Goldhaber, *Extended Abstracts: International Field Conference on Carbonate-Hosted Lead–Zinc Deposits*, Society of Economic Geologists, 1995, 358.
75 T. D. Branam and E. M. Ripley, Genesis of sediment-hosted copper mineralization in south-central Kansas: Sulfur/carbon and sulfur isotope systematics, *Econ. Geol.*, 1990, **85**, 601–621.
76 T. H. Giordano, Metal transport in ore fluids by organic ligand complexation, in *Organic Acids in Geological Processes*, ed. E. D. Pittman and M. D. Lewan, Springer-Verlag, New York, 1994, pp. 319–354.
77 G. M. Anderson, The hydrothermal transport and deposition of galena and sphalerite near 100 °C, *Econ. Geol.*, 1973, **68**, 480–492.
78 P. D. Lundegard and Y. K. Kharaka, Distribution and occurrence of organic acids in subsurface waters, in *Organic Acids in Geologic Processes*, ed. E. D. Pittman and M. D. Lewan, Springer-Verlag, New York, 1994, pp. 40–69.

79 Y. K. Kharaka, P. D. Lundegard and T. H. Giordano, Distribution and origin of organic ligands in subsurface waters from sedimentary basins, *Rev. Econ. Geol.*, 2000, **9**, 119–131.
80 R. M. Smith, A. E. Martell and R. J. Motekaitis, *NIST Critically Selected Stability Constants of Metal Complexes Database. NIST Standard Reference Database 46*, National Institute of Standards and Technology, 1998, p. 40.
81 E. L. Shock and C. M. Koretsky, Metal–organic complexes in geochemical processes: Estimation of standard partial molal thermodynamic properties of aqueous complexes between metal cations and monovalent organic acid ligands at high pressure and temperatures, *Geochim. Cosmochim. Acta*, 1995, **59**, 1497–1532.
82 D. A. Sverjensky, E. L. Shock and H. C. Helgeson, Prediction of the thermodynamic properties of aqueous metal complexes to 1000 °C and 5 kb, *Geochim. Cosmochim. Acta*, 1997, **61**, 1359–1412.
83 P. Prapaipong, E. L. Shock and C. M. Koretsky, Metal–organic complexes in geochemical processes: Temperature dependence of the standard thermodynamic properties of aqueous complexes between metal cations and dicarboxylate ligands, *Geochim. Cosmochim. Acta*, 1999, **63**, 2547–2577.
84 R. E. Mesmer, C. S. Patterson, R. H. Busey and H. F. Holmes, Ionization of acetic acid in NaCl (aq) media: A potentiometric study to 573 K, *J. Phys. Chem.*, 1989, **93**, 7483–7490.
85 T. H. Giordano, Anglesite ($PbSO_4$) solubility in acetate solutions: The determination of stability constants for lead acetate complexes to 85 °C, *Geochim. Cosmochim. Acta*, 1989, **53**, 359–366.
86 Y. K. Kharaka, W. D. Gunter, P. K. Aggarwal, E. H. Perkins and J. D. DeDraal, SOLMINEQ. 88, A computer program for geochemical modeling of water–rock interactions, *United States Geological Survey Water-Resources Investigation Report 88-4227*, 1988, p. 420.
87 T. H. Giordano and S. E. Drummond, The potentiometric determination of stability constants for zinc acetate complexes in aqueous solutions to 295 °C, *Geochim. Cosmochim. Acta*, 1991, **55**, 2401–2415.
88 R. M. Kettler, D. J. Wesolowski and D. A. Palmer, Dissociation quotients of malonic acid in aqueous sodium chloride media to 100 °C, *J. Solution Chem.*, 1992, **21**, 883–900.
89 A. Hammam, A. Olin and P. Svanstrom, The complex formation between Pb^{2+} and dicarboxylic acids $(CH_2)_n(COOH)_2$ with $n = 1$–4, *Acta Chem. Scand. Ser. A*, 1977, **31**, 384–390.
90 C. E. Evans and C. B. Monk, EMF studies of electrolytic dissociation. Part 10. Association constants of some zinc dicarboxylates in water, *Trans. Faraday Soc.*, 1970, **66**, 1491–1497.
91 W. Liu, D. C. McPhail and J. Brugger, An experimental study of copper(I) chloride and copper(I) acetate complexing in hydrothermal solutions between 50 °C and 250 °C and vapor-saturated pressure, *Geochim. Cosmochim. Acta*, 2001, **65**, 2937–2948.
92 A. E. Martell and R. M. Smith, *Critical Stability Constants 3. Other Organic Ligands*, Plenum Press, New York, 1977, p. 495.
93 A. E. Martell and R. M. Smith, *Critical Stability Constants 5. First Supplement*, Plenum Press, New York, 1982, p. 604.
94 R. M. Smith and A. E. Martell, *Critical Stability Constants 6. Second Supplement*, Plenum Press, New York, 1989, p. 643.
95 H. L. Barnes, Solubilities of ore minerals, in *Geochemistry of Hydrothermal Ore Deposits*, ed. H. L. Barnes, Wiley, New York, 2nd edn., 1979, pp. 405–461.
96 E. Roedder, *Fluid Inclusions, Reviews in Mineralogy*, Mineralogical Society of America, Washington, DC, 1984, vol. 12, p. 644.
97 H. Ohmoto; H. Ohmoto, Thermodynamic and kinetic evaluation of causes of metal-ratio regularities in low temperature hydrothermal deposits, *Annual Meeting of the Geological Society of America, Abstract with Programs*, 1985, 680.
98 G. Rittenhouse, R. B. Fulton, R. J. Grabowski and J. L. Bernard, Minor elements in oil-field waters, *Chem. Geol.*, 1969, **4**, 189–209.
99 G. K. Billings, B. Hitchon and D. R. Shaw, Geochemistry and origin of formation waters in the western Canada sedimentary basin, 2. Alkali metals, *Chem. Geol.*, 1969, **4**, 211–223.
100 B. Hitchon, G. K. Billings and J. E. Klovan, Geochemistry and origin of formation waters in the western Canada sedimentary basin-III. Factors controlling chemical composition, *Geochim. Cosmochim. Acta*, 1971, **35**, 567–598.
101 B. Hitchon, E. H. Perkins and W. D. Gunter, Recovery of trace metals in formation waters using acid gases from natural gas, *Appl. Geochem.*, 2001, **16**, 1481–1497.
102 A. G. Collins, *Geochemistry of Oilfield Waters*, Elsevier, New York, 1975, p. 496.
103 A. B. Carpenter and M. L. Trout, Geochemistry of bromide-rich brines of the Dead Sea and southern Arkansas, *Oklahoma Geol. Surv. Circ.*, 1978, **79**, 78–88.
104 Y. K. Kharaka, Origin and evolution of water and solutes in sedimentary basins, in *Hydrogeology of Sedimentary Basins: Applications to Exploration and Exploitation*, ed. B. Hitchon, S. Bachu and C. M. Sauveplane, *Proceedings of Third Canadian/American Conference on Hydrogeology*, National Water Well Association, Dublin, OH, 1986, pp. 173–195.
105 Y. K. Kharaka, A. S. Maest, T. A. Fries, L. M. Law and W. W. Carothers, Geochemistry of Pb and Zn in oil field brines: Central Mississippi Salt Dome Basin revisited, in *Proceedings, Conference on Genesis of Stratiform Sediment-Hosted Pb–Zn Deposits*, ed. R. J. W. Turner and M. T. Einaudi, Stanford University, 1986, pp. 181–187.
106 Y. K. Kharaka, A. S. Maest, W. W. Carothers, L. M. Law, P. J. Lamothe and T. L. Fries, Geochemistry of metal-rich brines from central Mississippi Salt Dome Basin, USA, *Appl. Geochem.*, 1987, **2**, 543–561.
107 L. S. Land, G. L. McPherson and L. E. Mack, The geochemistry of saline formation waters, Miocene, offshore Louisiana, *Gulf Coast Assoc. Geol. Soc. Trans.*, 1988, **38**, 503–511.
108 J. A. Saunders and C. T. Swann, Trace-metal content of Mississippi oil field brines, *J. Geochem. Explor.*, 1990, **37**, 171–183.
109 E. P. Moldovanyi and L. M. Walter, Regional trends in water chemistry, Smackover Formation, southwest Arkansas: Geochemical and physical controls, *Am. Assoc. Pet. Geol. Bull.*, 1992, **76**, 864–894.
110 J. R. Kyle, *The barite industry and resources of Texas, Bureau of Economic Geology, Mineral Resource Circular No. 85*, Bureau of Economic Geology, Austin, TX, 1994, 86 pp.
111 J. S. Hanor, Physical and chemical controls on the composition of waters in sedimentary basins, *Mar. Pet. Geol.*, 1994, **11**, 31–45.
112 J. S. Hanor, Variations in chloride as a driving force in siliciclastic diagenesis, in Siliciclastic Diagenesis and Fluid Flow: Concepts and Applications, *SEPM Spec. Publ. 55*, 1996, 4–12.
113 L. S. Land, Na–Ca–Cl saline formation waters, Frio Formation (Oligocene), south Texas, USA: Products of diagenesis, *Geochim. Cosmochim. Acta*, 1995, **59**, 2163–2174.
114 J. L. Palandri and M. H. Reed, Reconstruction of in situ composition of sedimentary formation waters, *Geochim. Cosmochim. Acta*, 2001, **65**, 1741–1767.
115 A. B. Carpenter, Origin and chemical evolution of brines in sedimentary basins, *Oklahoma Geol. Surv. Circ.*, 1978, **79**, 60–77.
116 Y. K. Kharaka, R. W. Hull and W. W. Carothers, Water–rock interactions in sedimentary basins, in *Relationships of Organic Matter and Mineral Diagenesis, SEPM Short Course 17*, ed. D. L. Gautier, Y. K. Kharaka and R. C. Surdam, Society of Economic Paleontologists and Mineralogists, 1985, pp. 79–176.
117 D. E. White, *Saline waters of sedimentary rocks, American Association of Petroleum Geologists Memoir 4*, American Association of Petroleum Geologists, 1965, pp. 342–366.
118 J. S. Hanor, Variations in the chemical composition of oil-field brines with depth in northern Louisiana and southern Arkansas: implications for mechanisms and rates of mass transport and diagenetic reaction, *Gulf Coast Assoc. Geol. Soc. Trans.*, 1984, **34**, 55–61.
119 K. M. McManus and J. S. Hanor, Diagenetic evidence for massive evaporative dissolution, fluid flow and mass transfer in the Louisiana Gulf Coast, *Geology*, 1993, **21**, 727–730.
120 T. P. Wilson and D. T. Long, Geochemistry and isotope chemistry of Ca–Na–Cl brines in Silurian strata, Michigan Basin, USA, *Appl. Geochem.*, 1993, **8**, 507–524.
121 P. K. Aggarwal, R. W. Hull, W. D. Gunter and Y. K. Kharaka, SOLMNEQF: A computer code for geochemical modeling of water–rock interactions in sedimentary basins, in *Hydrogeology of Sedimentary Basins: Applications to Exploration and Exploitation, Proceedings of Third Canadian/American Conference on Hydrogeology*, ed. B. Hitchon, S. Bachu and C. M. Sauveplane, National Water Well Association, Dublin, OH, 1986, pp. 196–203.
122 W. J. Wade, J. S. Hanor and R. Sassen, Controls on H_2S concentration and hydrocarbon destruction in the eastern Smackover trend, *Gulf Coast Assoc. Geol. Soc. Trans.*, 1989, **39**, 309–320.
123 E. L. Shock, Application of thermodynamic calculations to geochemical processes involving organic acids, in *Organic Acids in Geological Processes*, ed. E. D. Pittman and M. D. Lewan, Springer-Verlag, New York, 1994, pp. 270–318.
124 S. G. Franks, R. F. Dias, K. H. Freeman, J. R. Boles, A. Holba,

A. L. Finncannon and E. D. Jordan, Carbon isotopic composition of organic acids in oil field waters, San Joaquin Basin, California, USA, *Geochim. Cosmochim. Acta*, 2001, **65**, 1301–1310.
125 J. S. Seewald, Model for the origin of carboxylic acids in basinal brines, *Geochim. Cosmochim. Acta*, 2001, **65**, 3779–3789.
126 D. B. MacGown and R. C. Surdam, Difunctional carboxylic acid anions in oilfield waters, *Org. Geochem.*, 1988, **12**, 245–259.
127 Y. K. Kharaka, L. M. Law, W. W. Carothers and D. F. Goerlitz, Role of organic species dissolved in formation waters from sedimentary basins in mineral digenesis, in *Roles of Organic Matter in Sedimentary Digenesis, Society of Economic Paleontologists and Mineralogists Special Publication 38*, ed. D. L. Gautier, Society of Economic Paleontologists and Mineralogists, Tulsa, OK, 1986, pp. 111–128.
128 P. D. Lundegard and Y. K. Kharaka, Geochemistry of organic acids in subsurface waters-field data, experimental data, and models, in *Chemical Modeling of Aqueous Systems II, ACS Symp. Ser. 416*, ed. D. C. Melchoir and R. L. Bassett, 1990, pp. 169–189.